Wind Atlas for the Gulf of Suez Satellite Imagery and Analyses

Hasager, Charlotte Bay

Publication date:
2003

Document Version
Publisher's PDF, also known as Version of record

RISØ

Risø-I-1969(EN)

Wind Atlas for the Gulf of Suez
Satellite Imagery and Analyses

Charlotte B. Hasager

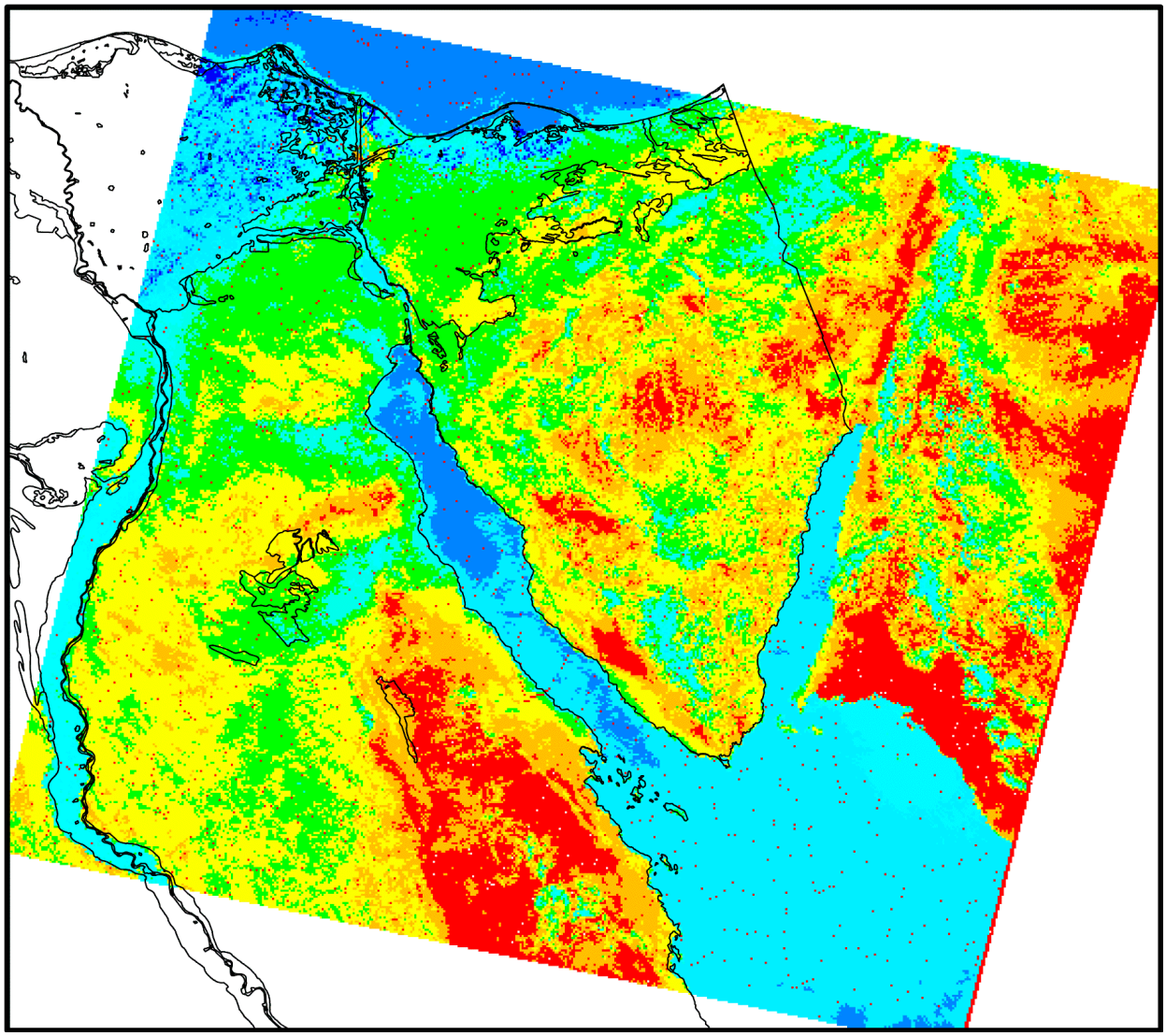

Risø National Laboratory, Roskilde, Denmark
April 2003

Risø-I-1969(EN)

Wind Atlas for the Gulf of Suez
Satellite imagery and analyses

Charlotte B. Hasager

Risø National Laboratory, Roskilde
April 2003

Abstract **S**atellite imagery and data have been used to investigate the spatial distributions of wind speed and some terrain surface characteristics in the Gulf of Suez. The methods and the results are described in three separate sections:

1. "Comparing SAR winds and in-situ winds". Synthetic Aperture Radar (SAR) data derived from the European Remote Sensing Satellite (ERS) have been used to make wind speed maps for the Gulf of Suez.
2. "Land cover from Landsat TM imagery". Landsat Thematic Mapper (TM) data have been used to establish true- and false-colour land cover maps, as well as land cover classification maps.
3. "Reporting on satellite information for the Wind Atlas for Egypt". Along-Track Scanning Radiometer (ATSR) data from the European Remote Sensing Satellite (ERS) have been used to map the sea- and land-surface temperatures and albedos.

The present report is a result of the Egyptian-Danish project *Wind Atlas for Egypt*. This project and the publication of the report are funded by the Danish Ministry of Foreign Affairs through Danida.

Print: Pitney Bowes Management Services Danmark A/S, 2003

Wind Atlas for the Gulf of Suez
Comparing SAR winds and in-situ winds

1 Site description

The Gulf of Suez in Egypt has for many years been investigated in regard to the wind resources (Mortensen and Said, 2002). The wind resources are very good due to the regional weather systems given generally high wind power potentials. So far a wind farm at Zafarana has been installed on land and more are being planned. A number of meteorological masts have been operated for several years. Currently 12 are in operations. Comparison to these data may offer a unique opportunity. Below is given the results of three cases where SAR wind speed maps are compared to meteorological observations.

1.1 Comparison of SAR scenes and WAsP results

To assess spatial features of the wind climate in the Gulf of Suez, three cases are studied from satellite images. The ERS SAR satellite data from ESA (European Space Agency; AO3-153) are analysed for wind speeds over the ocean. The C-band radar signals are processed with the CMOD-IFRE2 by NERSC (Nansen Environmental Remote Sensing Centre) in Bergen, Norway (Hasager et al. 2001).

Case I: 5 April 1996

The first case is from 5 April 1996 at 20.10 UTC. Three satellite scenes, each 100 km * 100 km large covers the Gulf of Suez. The original cell resolution in the images is 25 m * 25 m. However, to avoid so-called speckle noise, the image data has been regridded into a 400 m * 400 m cell size. The wind speed is calculated for 10 m above the ocean assuming the wind direction to be constant at 20º as measured in Zafarana (see Table 1). The processed data are shown in Figure 2. It is possible to see two thin lines across the Gulf (the upper line is near Zafarana). It is a technical artifact of the mosaic of three satellite scenes.

Meteorological observations are available from three masts near the coast: in the north Abu Darag and Zafarana and in the south Gulf of El-Zayt. The observations are graphed in Figure 1 and listed in Table 1. At the 25 m level the wind speeds in Abu Darag is 15.7 m s^{-1}, in Zafarana 18.8 m s^{-1} and in Gulf of El-Zayt only 5.3 m s^{-1}. This indicates a north-south gradient decreasing from the north towards south. In the satellite image a similar trend is observed. In the northern part of the Gulf strong winds occur and lower winds in the southern part.

For comparing the mast observations over land to the 10 m wind over sea, the WAsP model has been used. The results of the of WAsP calculated wind speeds at 10 m level above the sea is listed in Table 1 together with the SAR wind speed observations. The comparison shows that the SAR wind speeds are very much lower than the observations. Near Gulf of El-Zayt the SAR wind speed map shows values below 2 m s^{-1} which is below the validity range of SAR for wind speed mapping. For the Abu Darag and Zafarana sites it is not clear why the differences of up to 10 m s-1 can

appear between observations and the SAR wind speed map. The atmospheric flow was stationary prior to the satellite overpass as shown in Figure 1 so it cannot be due to e.g. frontal activity. Uncertainty on wind direction in the SAR algorithms could not lead to errors of this magnitude. No conclusion is found and further analysis is needed.

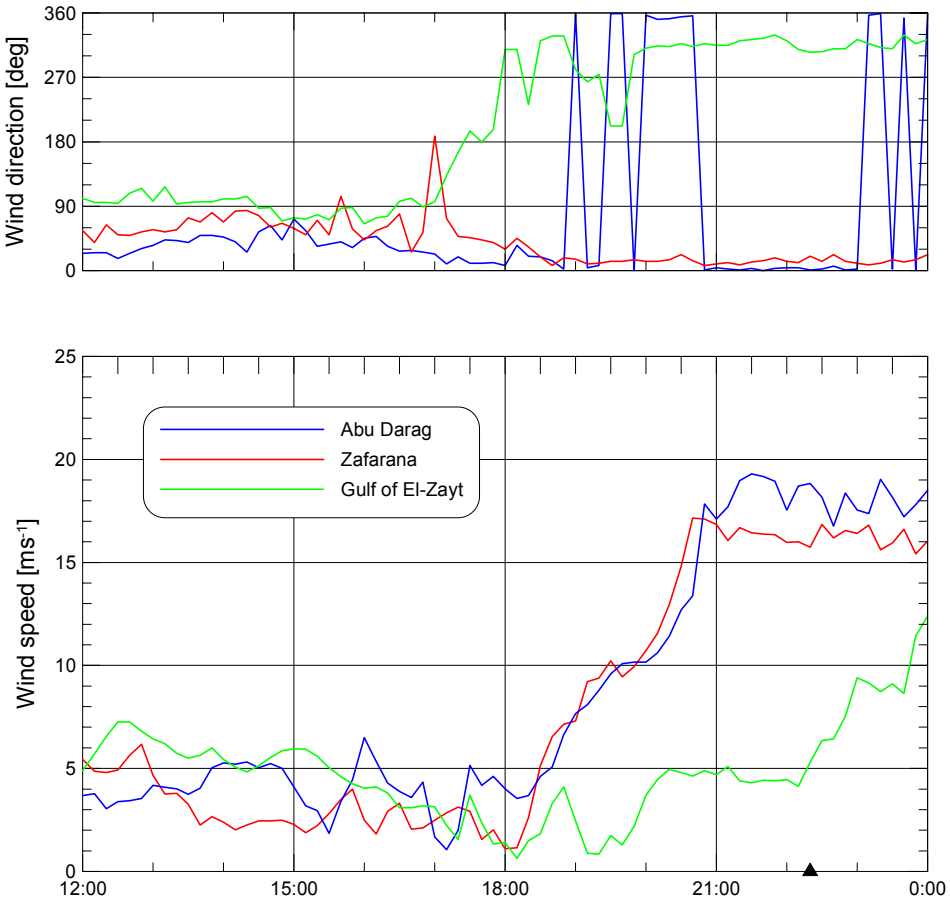

Figure 1. Meteorological data from Abu Darag, Zafarana and Gulf of El-Zayt on the5 April 1999. The ERS SAR overpass time is indicated with a '▲'

Table 1. Observations and predictions for 5 April 1996: site name, measured mean wind speed U *at 24.5 m a.g.l., wind direction* D *and temperature* T. *Estimated wind speed* U_e *and direction* D_e *at 10 m a.s.l., about 5 km offshore.* U_{SAR} *is from the SAR wind speed map.*

Met. station	*U*	*D*	*T*	U_e	D_e	U_{SAR}
	[m s^{-1}]	[°]	[°C]	[m s^{-1}]	[°]	[m s^{-1}]
Abu Darag	15.74	001	19.6	15.66	001	6.3
Zafarana	18.83	020	19.8	18.45	020	7.5
Gulf of El-Zayt	5.30	305	22.9	6.25	305	1.5

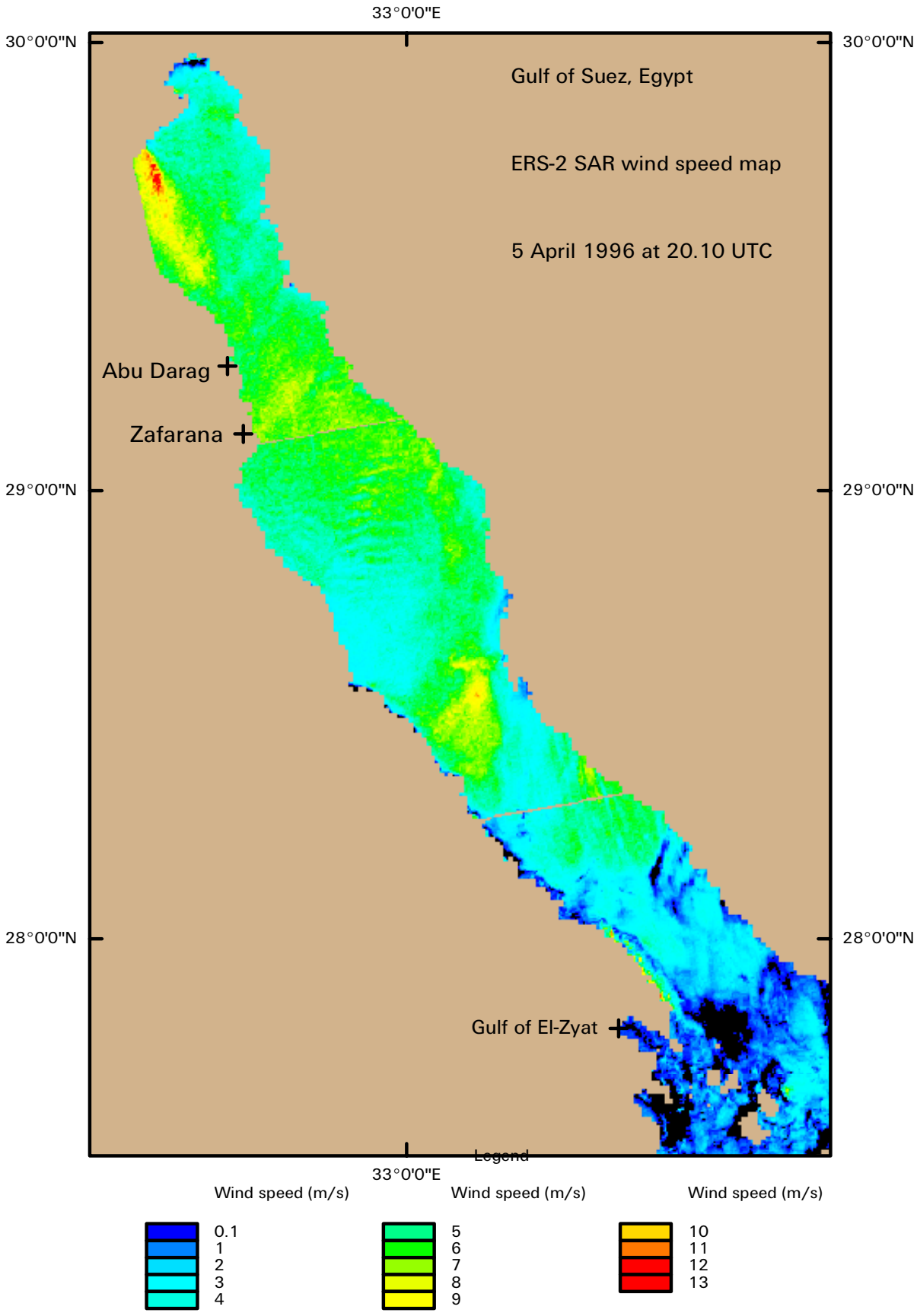

Figure 2. ERS SAR wind speed map of Gulf of Suez, Egypt . 5 April 1996 at 20.10 UTC. Courtesy of Birgitte Furevik, NERSC.

Case II: 2 October 1999

The second case is from 2 October 1999 at 20.07 UTC. It covers only the southern part of the Gulf of Suez and part of the Red Sea. The ERS SAR wind speed map is shown in Figure 4 calculated for a wind direction of 246º. Meteorological observations from Hurghada at the time of the satellite overpass are shown in Figure 3 and Table 2. Streaks in the image data shows the wind direction is from the North. A local maximum in wind speed around 10 m s^{-1} is found North of the Gulf of El-Zayt. Hurghada is located 10 km south of the image. WAsP has been used to calculate the local wind speed at 10 m above sea level 5 offshore from Hurghada. This result and SAR wind speed observations in the southern part of the image are compared in Table 2. It is seen that the SAR wind speed of 3.8 m s^{-1} is lower than the estimated wind speed of 5.0 m s^{-1}. But as may be noted in the image (Figure 4) winds up to 6.4 m s^{-1} are also found in the southern part of the image. Local wind gradients within few kilometer could also be found further south.

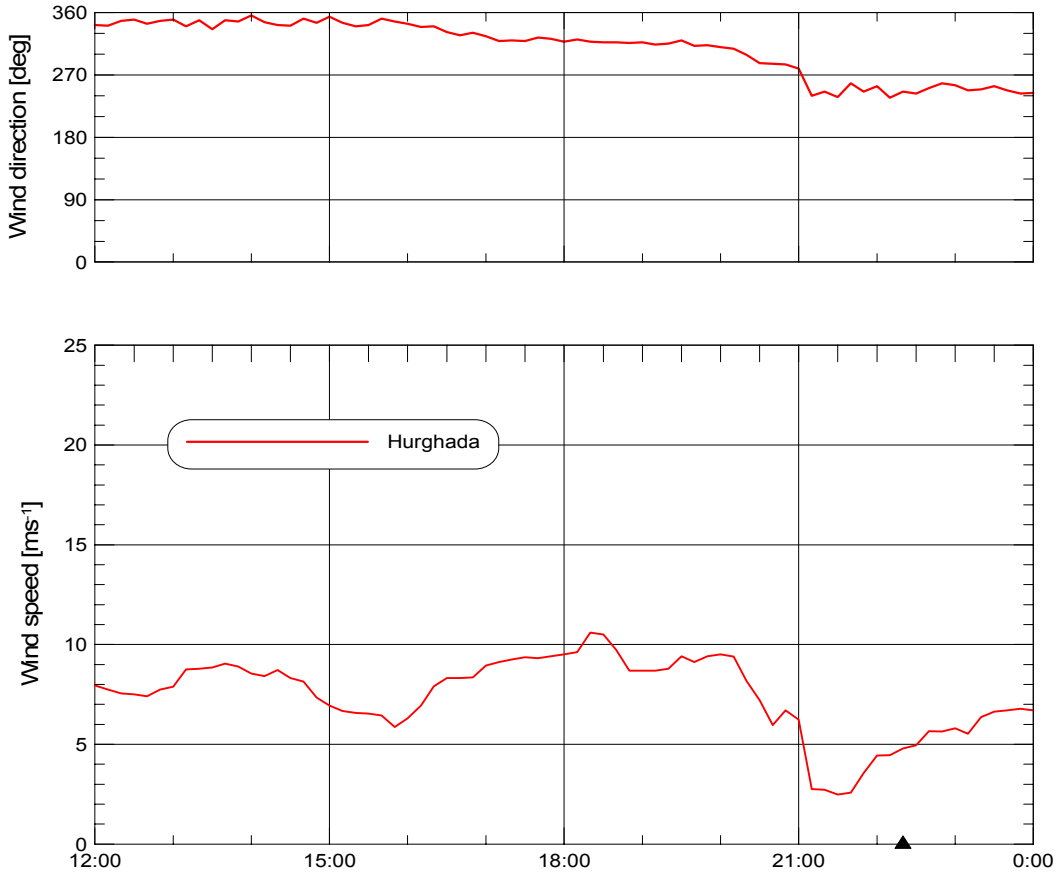

Figure 3. Meteorological data from Hurghada on the 2 October 1999. The ERS SAR overpass time is indicated with a '▲'

Table 2. Observations and predictions for 2 October 1999: site name, measured mean wind speed U *at 24.5 m a.g.l., wind direction* D *and temperature* T. *Estimated wind speed* U_e *and direction* D_e *at 10 m a.s.l., about 5 km offshore* U_{SAR} *is from the SAR wind speed map.*

Met. station	*U*	*D*	*T*	U_e	D_e	U_{SAR}
	[m s^{-1}]	[°]	[°C]	[m s^{-1}]	[°]	[m s^{-1}]
Hurghada	4.80	246	27.8	5.08	246	3.8

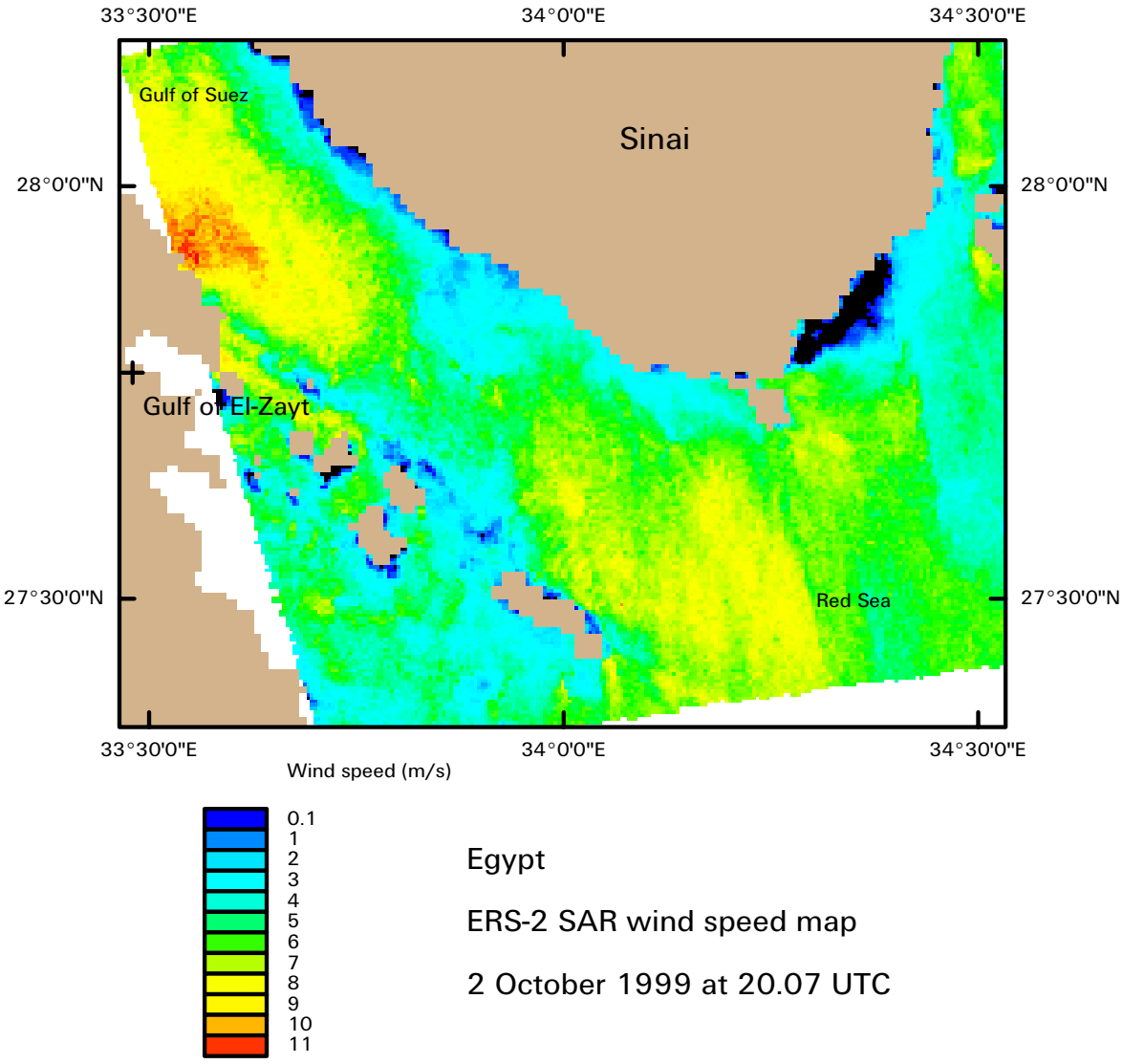

Figure 4. ERS SAR wind speed map of Gulf of Suez, Egypt. 2 October 1999 at 20.07 UTC. Courtesy of Birgitte Furevik, NERSC.

Case III: 10 November 1999

The third case is from 10 November 1999 at 20.13 UTC. It is a scene from the middle part of the Gulf of Suez (Figure 6). The meteorological observation at Zafarana at 24.5 m is a wind speed of 4.57 m s^{-1}. The daily observations are given in Figure 5. The wind direction is from the west. This wind direction was used in the SAR wind speed algorithm. WAsP has been used to calculate the 10 m sea level wind speed and the result is shown in Table 3 and compared to the observations in the SAR wind speed map. There is a strong wind gradient from 5.3 m s^{-1} to 2.5 m s^{-1} i.e. average 3.9 m s^{-1} at a distance of 5 km offshore from Zafarana. The result compares reasonably.

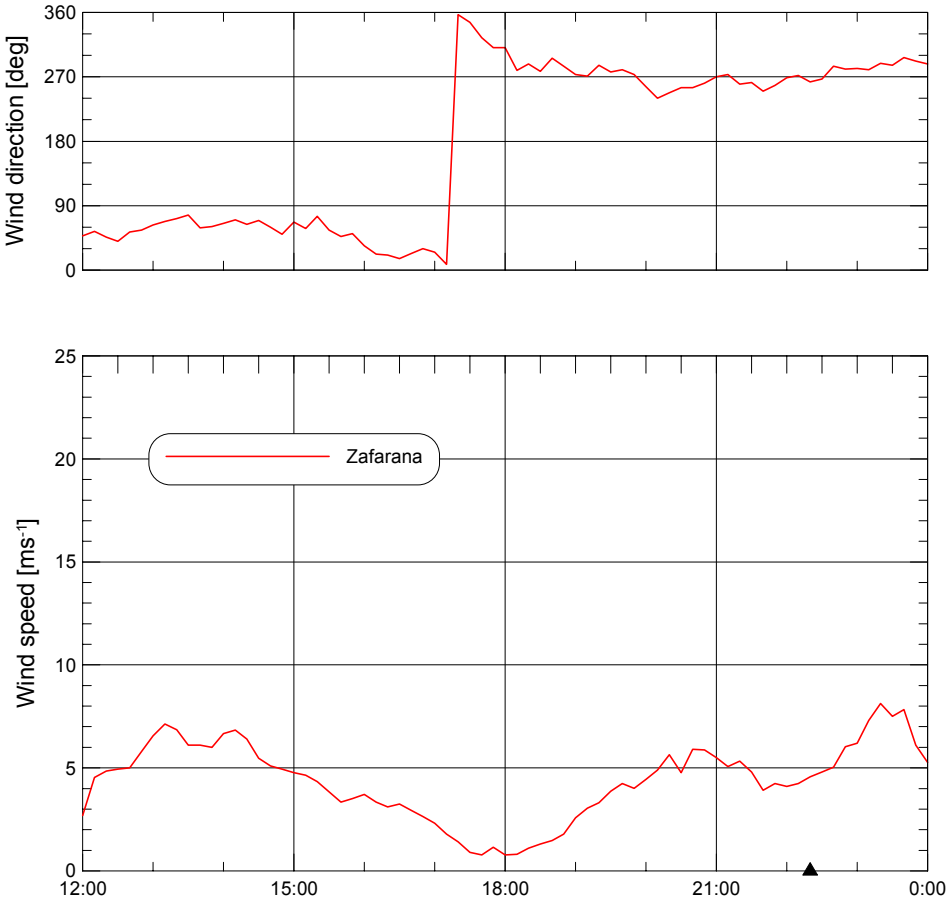

Figure 5. Meteorological data from Zafarana on the 10 November 1999. The ERS SAR overpass time is indicated with a '▲'

Table 3. Observations and predictions for 10 November 1999: site name, measured mean wind speed U *at 24.5 m a.g.l., wind direction* D *and temperature* T. *Estimated wind speed* U_e *and direction* D_e *at 10 m a.s.l., about 5 km offshore.* U_{SAR} *is from the SAR wind speed map.*

Met. station	*U*	*D*	*T*	U_e	D_e	U_{SAR}
	[m s^{-1}]	[°]	[°C]	[m s^{-1}]	[°]	[m s^{-1}]
Zafarana	4.57	263	18.1	5.03	263	3.9

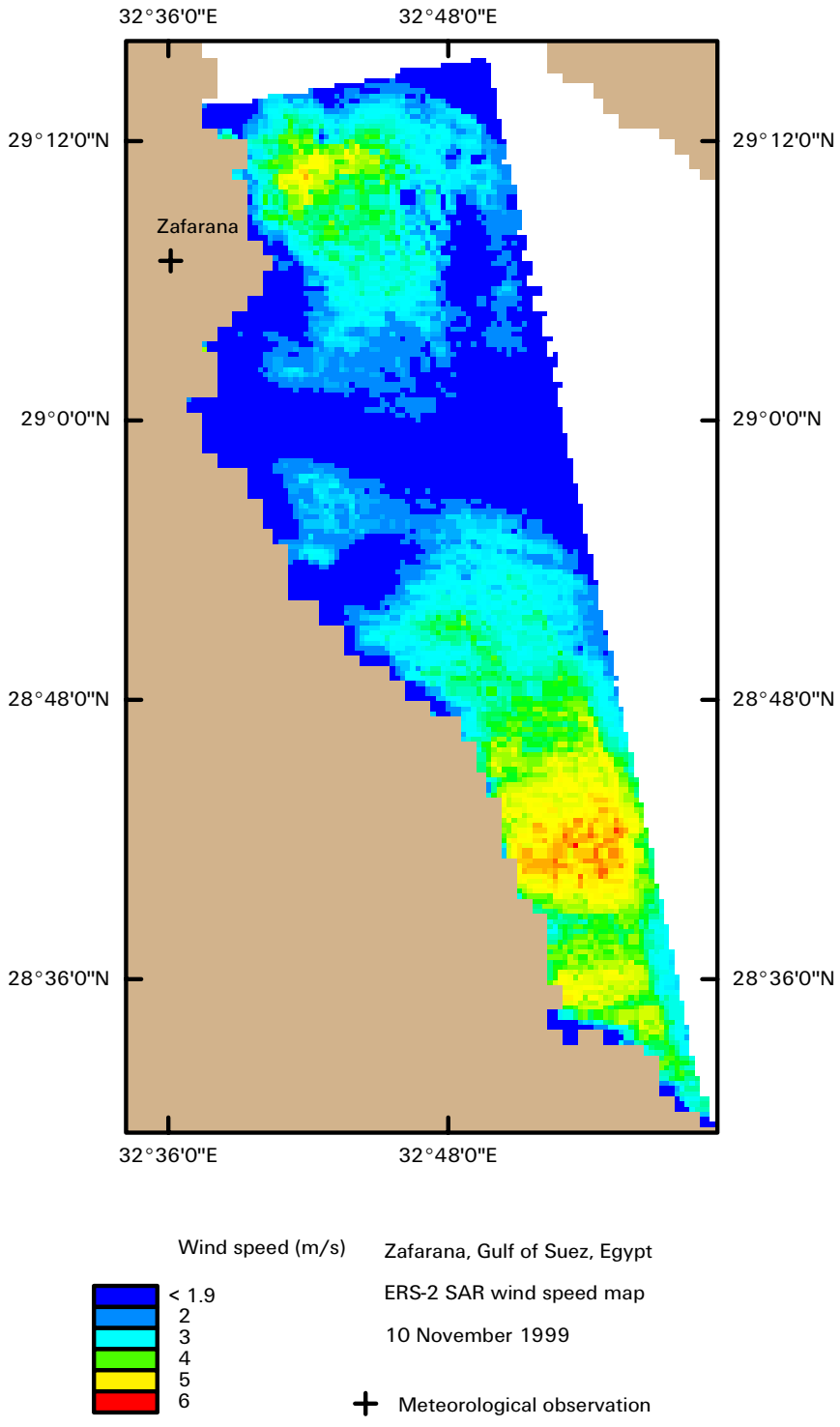

Figure 6. ERS SAR wind speed map of Gulf of Suez, Egypt. 10 November 1999 at 20.13 UTC. Courtesy of Birgitte Furevik, NERSC.

Linear correlation analysis between the WAsP wind speed results at 5 km offshore distance and the SAR wind speed maps is shown in Figure 7. All SAR wind speeds are systematically lower than the WAsP wind speed. For two observations the differences are as much a 10 m s^{-1}, for one observation 5 m s^{-1} and for two observations only 1.3 m s^{-1}. The data set is rather small and no clear conclusions can be made. Validation studies are challenging in the Gulf of Suez due to the pronounced spatial wind speed gradients in all the SAR scenes. Meteorological observations at coastal stations may be difficult to extrapolate far offshore.

In the current study the wind direction from the meteorological masts have been used at input to the CMOD-IFR algorithm. It may be an advantage to input the wind direction that can be retrieved directly from the SAR images themselves by two-dimensional Fourier Transforms or wave-let analysis.

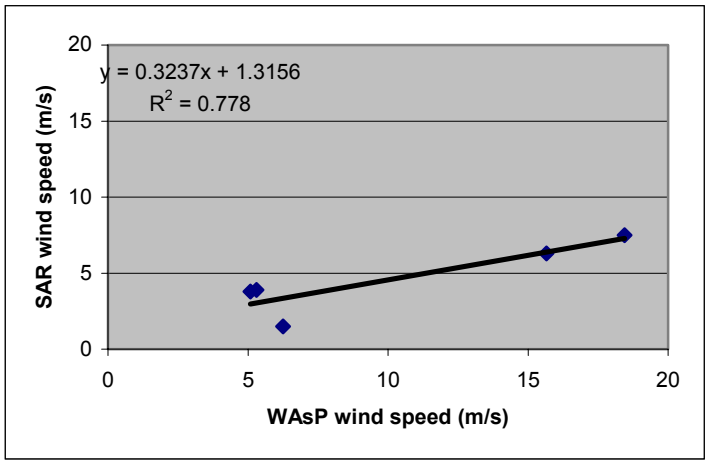

Figure 7. Linear correlation between wind speed from WAsP 5 km offshore and SAR wind speed observations.

1.2 Summary on offshore wind speeds in the Gulf of Suez

The SAR wind speed maps for the Gulf of Suez area in Egypt have been retrieved from the CMOD-IFR2 model with input of wind direction from local in-situ observations collected at the coast. The SAR scenes map only three cases, hence no clear statistically-based conclusions can be made. The finding though is that the SAR wind speed maps shows lower values compared to the wind speeds offshore is calculated by WAsP model. Validation studies are challenging in the Gulf of Suez due to the pronounced spatial wind speed gradients that are obvious in all three cases.

References

Hasager, C.B., Furevik, B., Dellwik, E., Sandven, S. Frank, H.P., Jensen, N.O., Astrup, P., Joergensen, B.H., Rathmann, O., Barthelmie, R.; Johannessen, O., Gaudiosi, G.; Christensen, L.C., 2001 Satellite images used in offshore wind resource assessment. 2001 Eds. P.Helm and A. Zervos. *Proceedings of the European Wind Energy Conference and exhibition (EWEC), Copenhagen (DK), 2-6 July 2001, 673-677*, See proceedings

Mortensen, N. G. and Said, U. S.: 2002, 'Wind Atlas for the Gulf of Suez. Measurements and Modelling 1991-1995'**ISBN87-550-2143-3**, 1-110

Acknowledgements. The ERS SAR scenes are granted from ESA AO3-153.

Charlotte Bay Hasager and Niels G. Mortensen, Risø, National Laboratory, May 2002.

Wind Atlas for the Gulf of Suez
Land cover from Landsat TM imagery

Satellite land cover maps

Land surface maps for Gulf of Suez are investigated from Landsat TM satellite data. One full scene from 7 April 1996 at 07:26 UTC and a quarter scene from 29 Mars 1996 at 07:32 UTC are used for the analysis.

The scenes are geometrically corrected image-to-image to a NOAA AVHRR satellite scene and vector layers from Digital Chart of the World (DCW) in a latitude-longitude grid. The scenes are mosaiced into one image. The pixel resolution is 30 m * 30 m and the area covered is approximately 150 km long and 100 km wide (Fig. 1). Fig. 1 is shown in false colour, i.e. near-infrared (ch 4) is loaded in RED, red (ch 3) in GREEN and green (ch 2) in BLUE. It is easy to see structures like mountains and the Nile. At Zafarana and Gulf of El-Zayt two zoom-in images are shown (Fig. 2). Here it is also possible to see road structures and different landscapes.

In order to use the information an unsupervised classification analysis is performed. In Fig. 3-5 the results for three sites, Abu Darag, Zafarana and Gulf of El-Zayt are shown. The positions of the meteorological masts are indicated. At this time the 12 classes are not given names, only numbers. Through a field survey the classes could be given appropriate names. This could also include relevant roughness values.

At a local area near Gulf of El-Zayt a supervised classification analysis is performed. It means that geomorphological units that are visible to the image analysist are used as training areas for the classification. The result is shown in Fig. 6. A similar procedure is used for the Zafarana – Abu Darag and the result is shown in Fig. 7. For the whole Gulf of Suez area, an unsupervised classification was run and the vegetation was identified separately from NDVI values. The result is shown in Fig. 8. The result is only indicative and field surveys or other observations should be used to assess the accuracy of the results before use.

Acknowledgements

The Landsat TM scenes are from Ornis Consult.

Dr. Charlotte Bay Hasager
Risø National Laboratory
9 August 2001

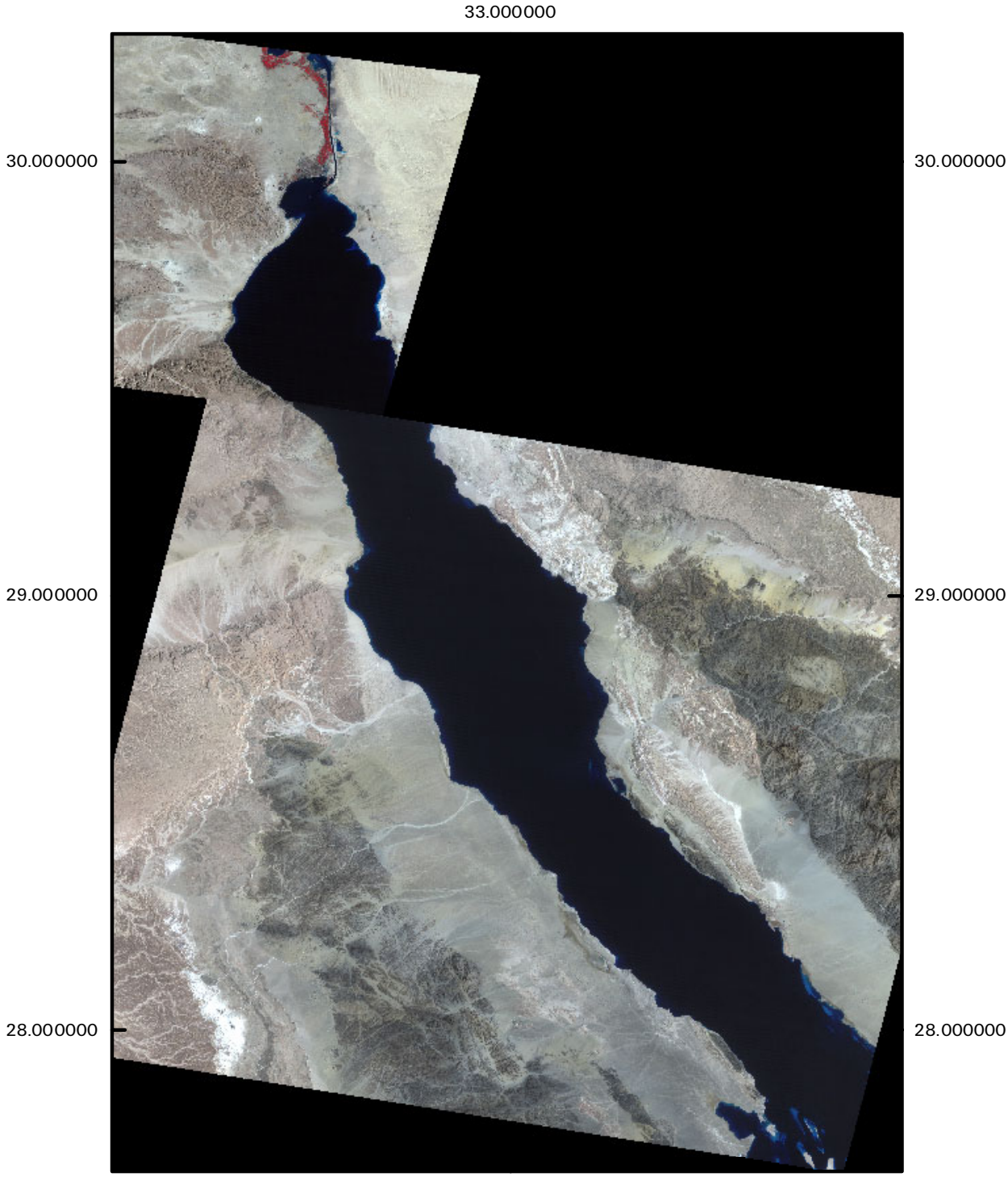

Fig. 1. Gulf of Suez true-color map from Landsat TM 7 April and 29 Mars 1996.

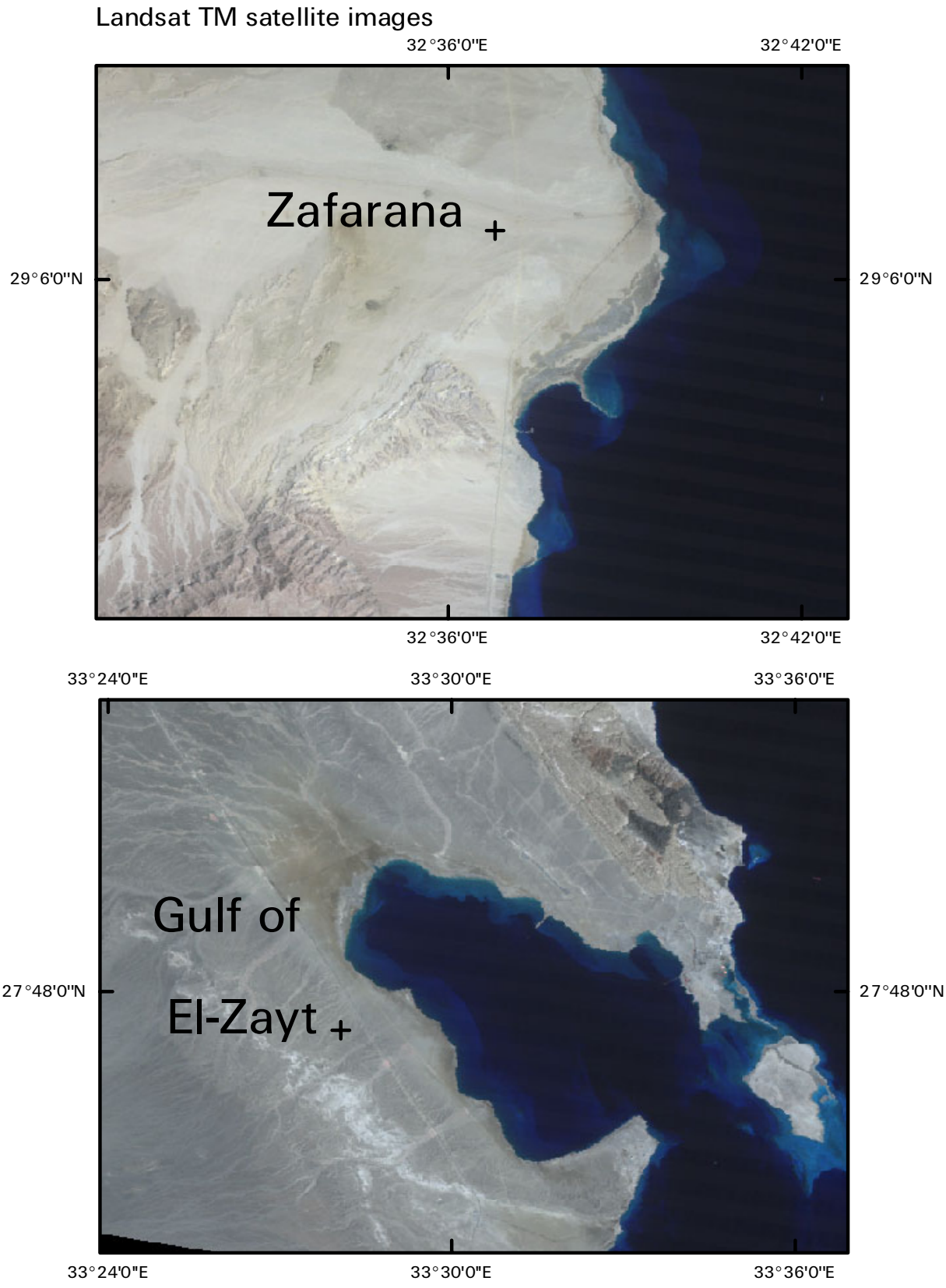

Fig. 2. Zafarana and Gulf of El-Zayt area from Landsat TM in true-color 7 April 1999.

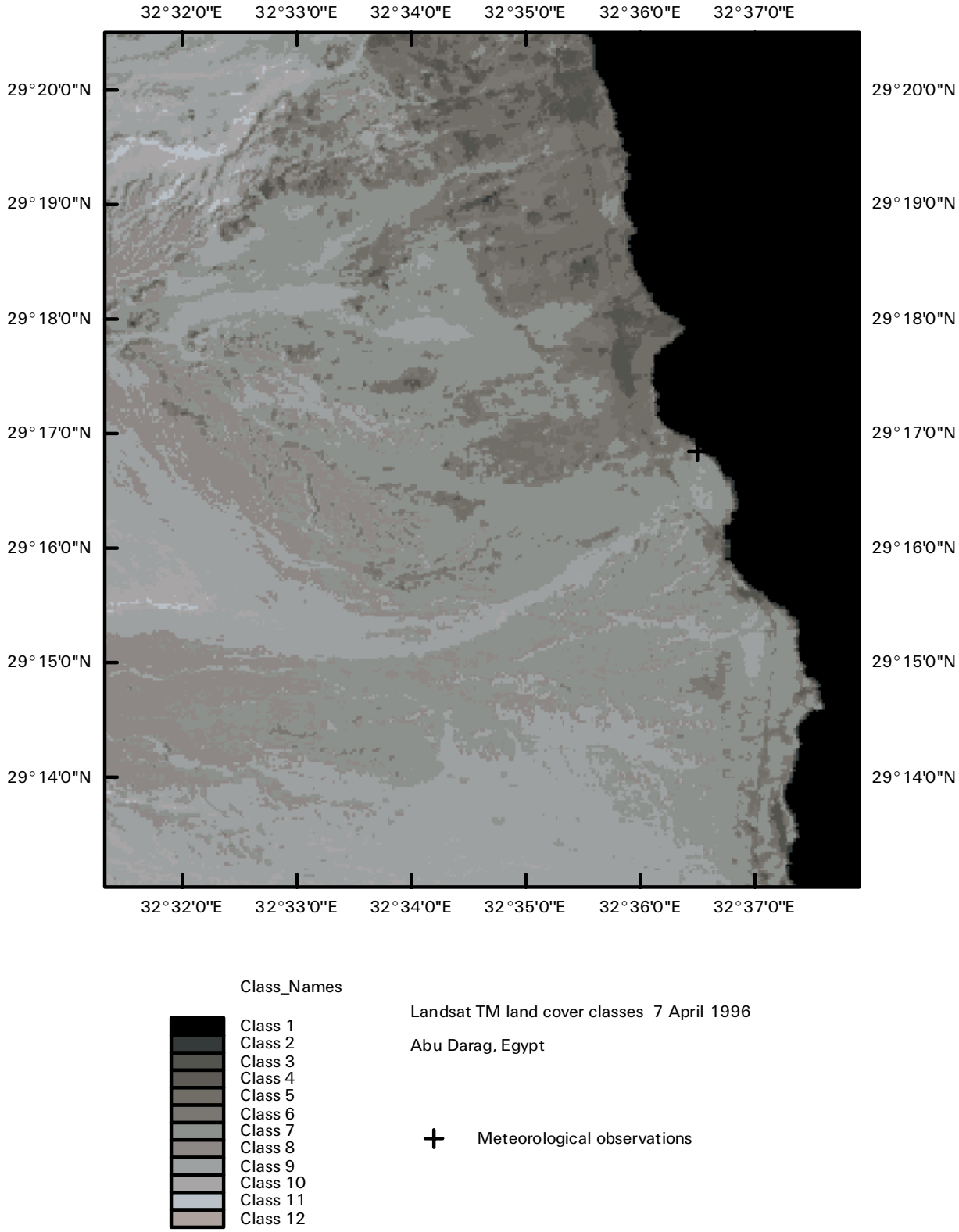

Fig. 3. Abu Darag area in Egypt from Landsat TM in true-color 7 April 1996.

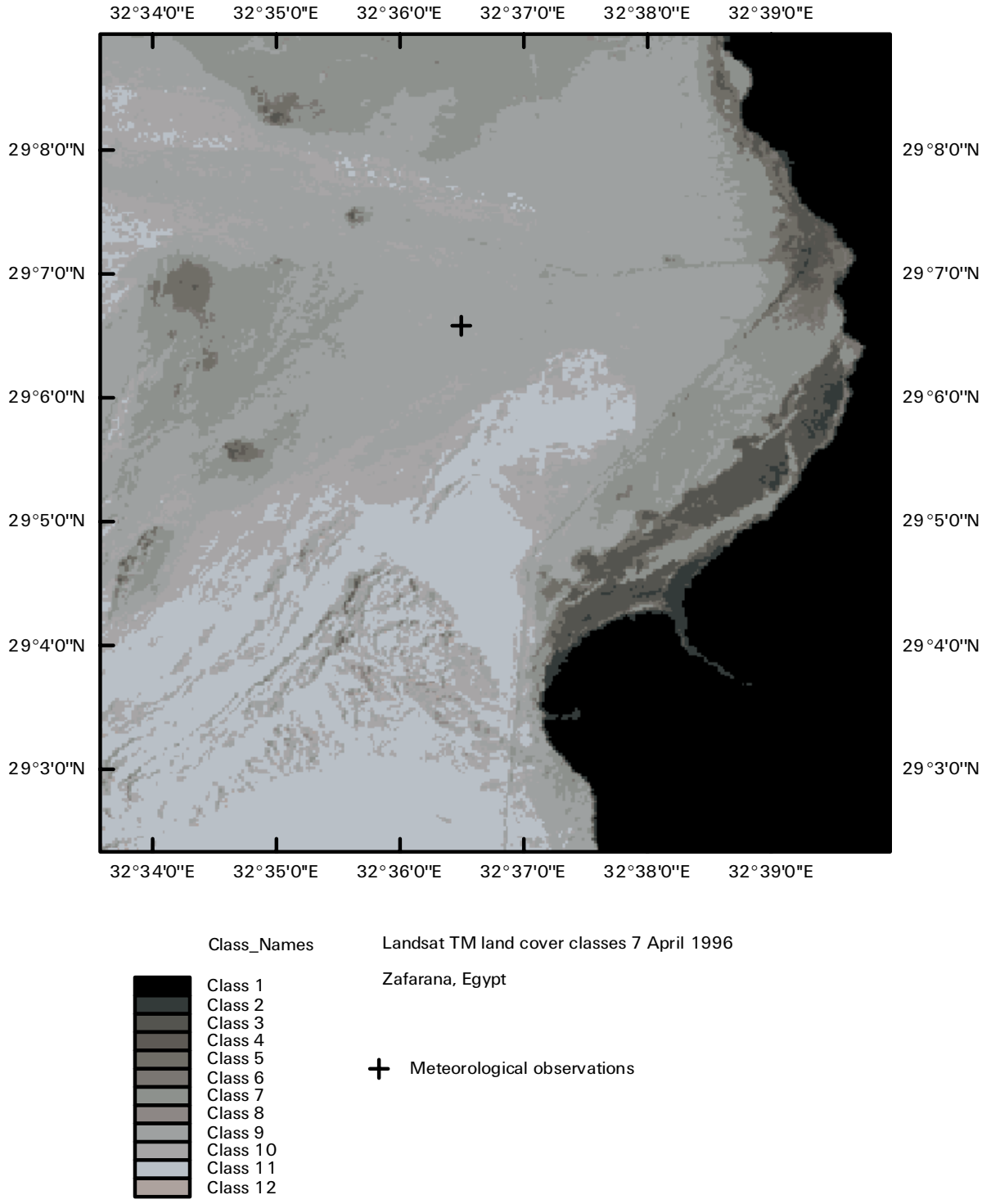

Fig. 4. Zafarana, Egypt from Landsat TM classification. 7 April 1996.

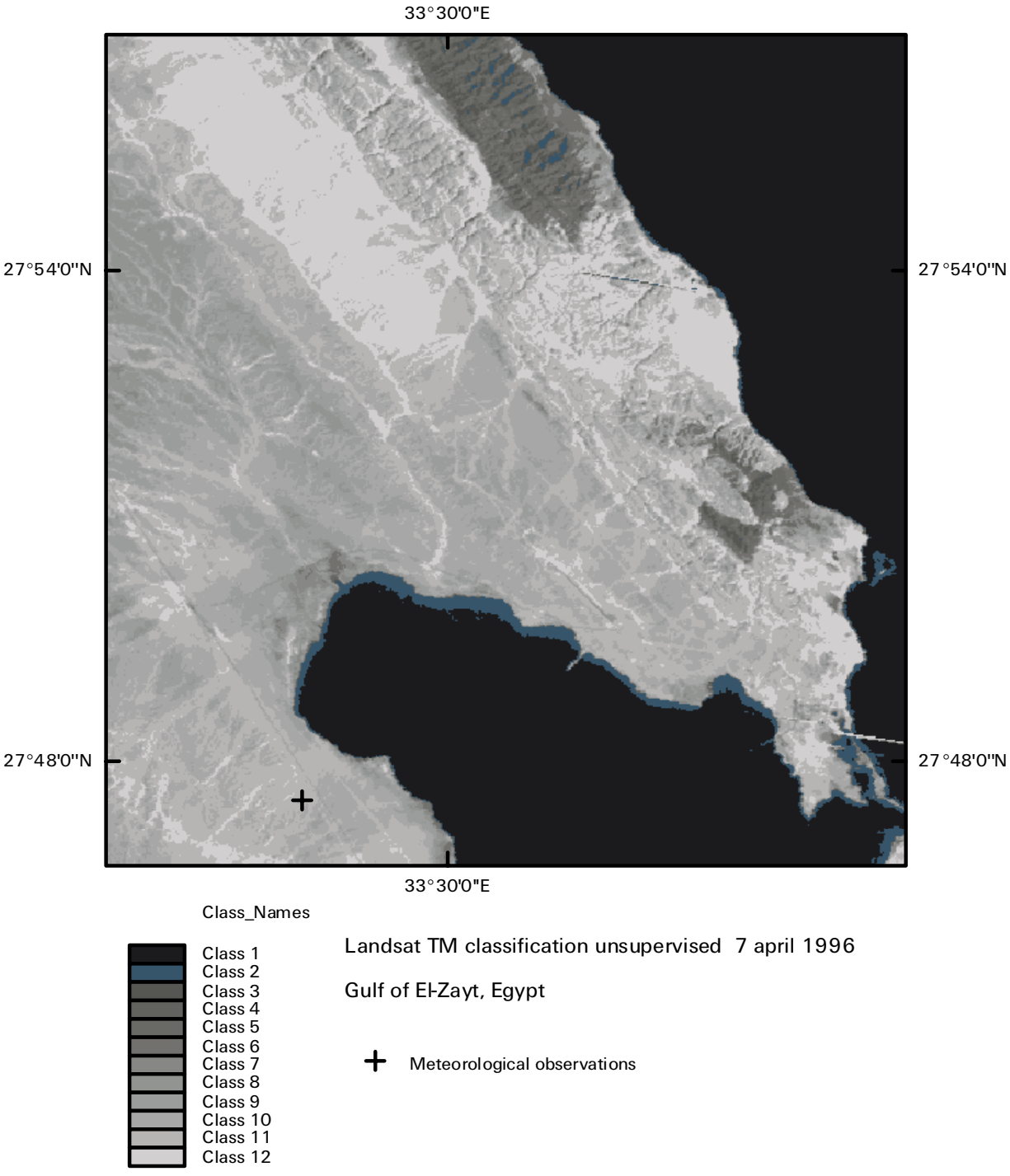

Fig. 5. Gulf of El-Zayt, Egypt from Landsat TM. Classification 7 April 1996.

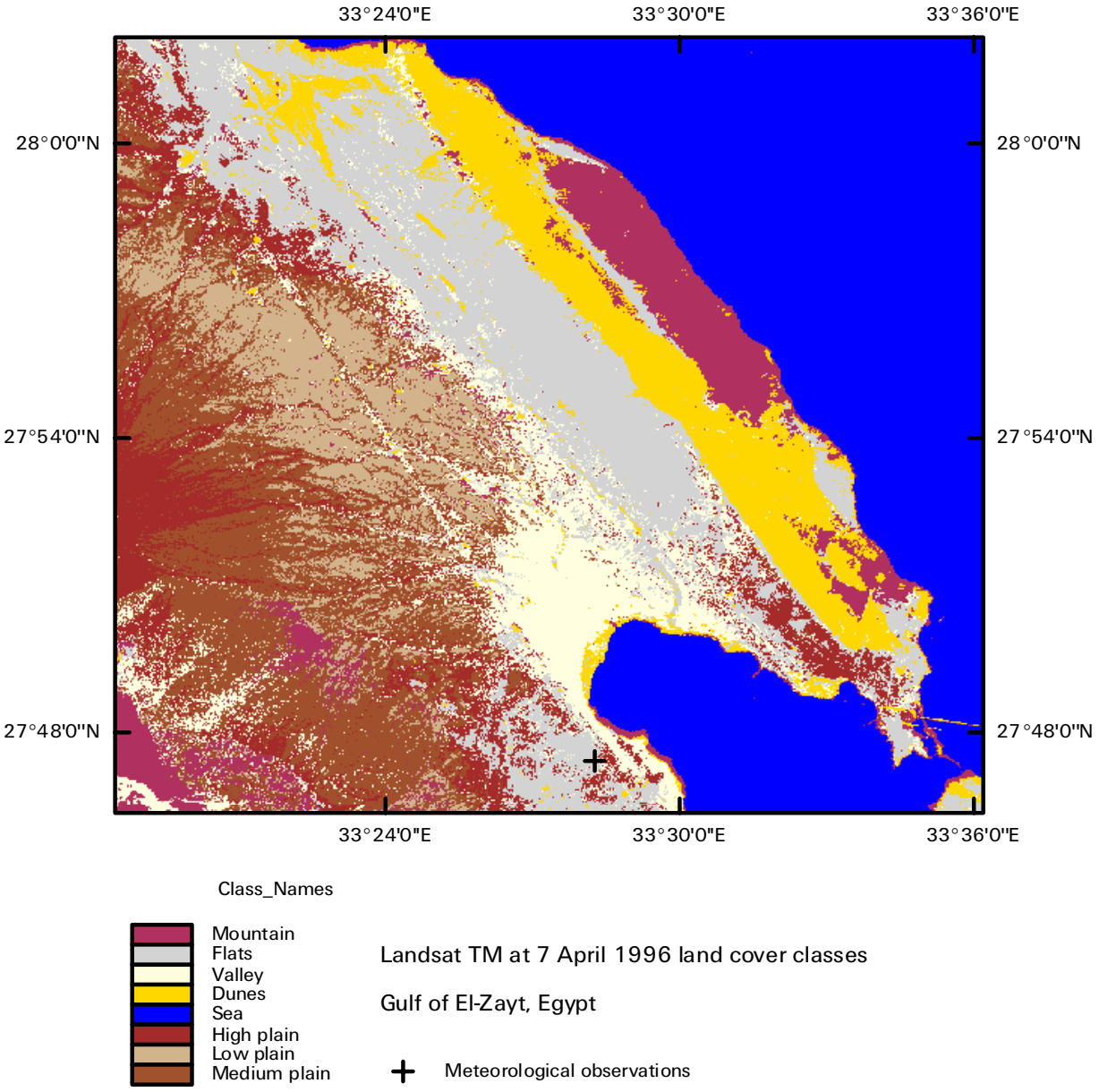

Fig. 6 Gulf of El-Zayt, Egypt from Landsat TM. Classification with class names 7 April 1996.

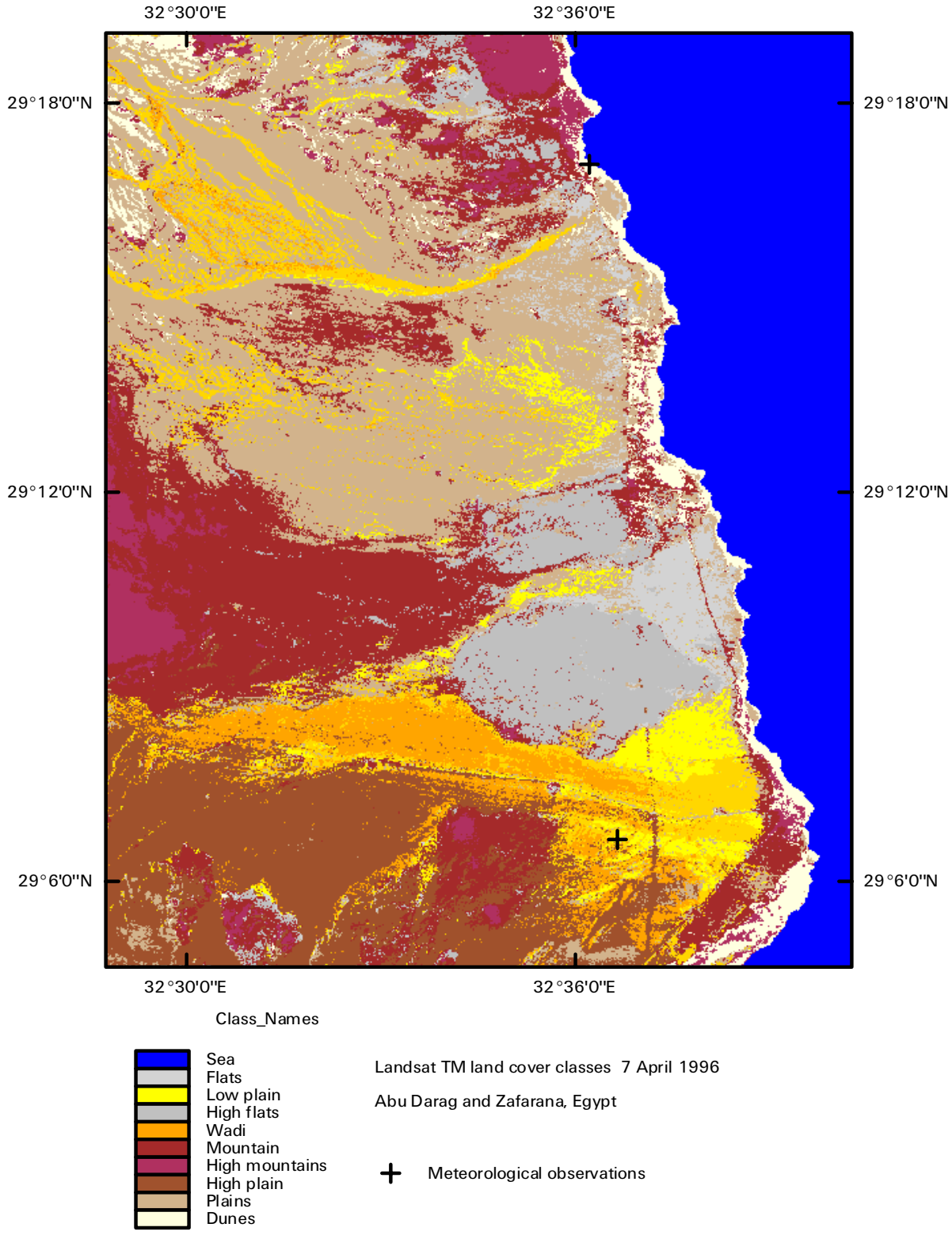

Fig. 7. Zafarana, Egypt from Landsat TM classification with class names 7 April 1996.

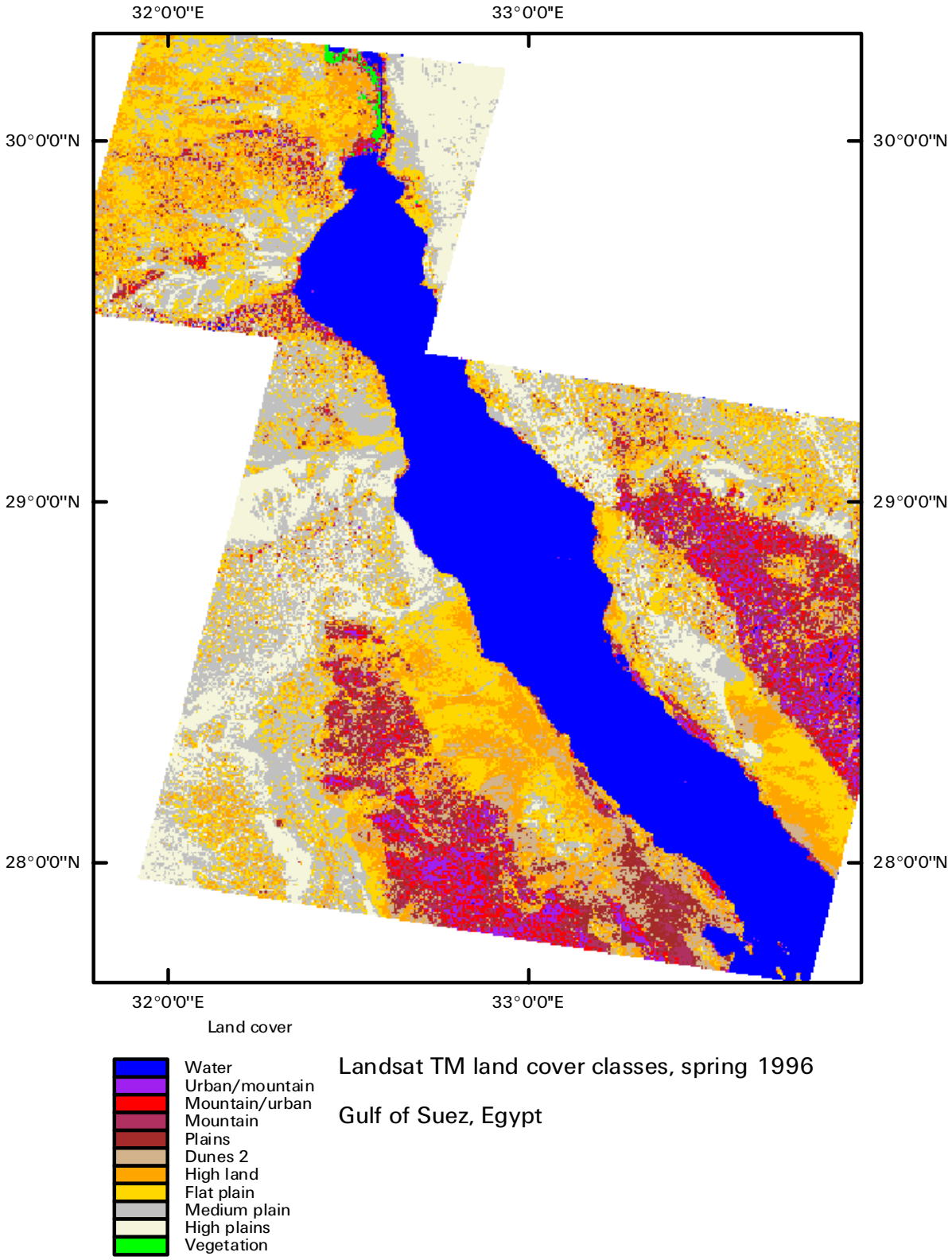

Fig. 8. Gulf of Suez, Egypt from Landsat TM classification with class names / April – 29 Mars 1996.

Intentionally left blank

Charlotte Bay Hasager
Risø National Laboratory
Wind Energy and Atmospheric Physics Dept.
Denmark
25 October 1999

Reporting on satellite information for the Wind Atlas for Egypt

Introduction

Information on land and sea surface temperatures, albedo and roughness can be retrieved from satellite scenes. The current report concerns land and sea surface temperatures and albedo retrieved in the Gulf of Suez area and in Egypt.

In the Wind Atlas for Egypt project satellite information is relevant for two things. One is as input to the KAMM model calculating the mesoscale atmospheric situations at regional scale. The other is as input to the WasP model calculating the wind energy potential of siting wind turbines at any location, i.e. local scale.

In the investigation of the atmospheric circulation it is of interest to have scenes from all seasons, morning and evening. Wind speeds are maximum in June and August/September. In winter the wind speeds are lower and rather constant with a minimum in December. At the daily time scale wind speed peaks in the evening, generally.

Migrating birds in very great numbers pass the Gulf of Suez area in September (southern migration) and again in March/April (northern migration). In September e.g. storks will cross around 10.00-11.00 AM. These storks typically will arrive very close to the surface on the western banks of the Gulf of Suez. Other birds migrate at night and at much higher levels.

Description of the ERS-2 ATSR satellite scenes

19 satellite scenes from ERS-2 ATSR are processed and analyzed. Two extra ATSR scene are ordered (per 21-10-1999). All the ATSR scenes are granted within the ERS-AO3 (**A**nnouncement of **O**pportunity) call. This means they are free of cost. The chosen scenes are (near) cloud free. Cloud cover is not a serious problem in Egypt.

ERS-2 (**E**uropean **R**emote sensing **S**atellite) is owned by the European Space Agency (ESA). The satellite was launched in September 1995. It is still in operation. On-board ERS-2 are two sensors of interest for the current project: ATSR (Along-Track Scanning Radiometer) and SAR (Synthetic Aperture Radar). Only the ATSR scenes are described here. In a later report the SAR scenes will be described. The SAR scenes analysis will focus on roughness mapping at local to regional scale.

ERS-2 is in a near-polar, sun-synchron orbit. This means that the satellite records the same location on earth at the same time of the day. For Egypt the ERS satellite descends in the morning around 8.00 UTC and ascends in the evening around 20.00 UTC. This corresponds to 10.00 and 22.00 local time.

For the Gulf of Suez area a suite of 6 morning and 5 evening scenes are chosen. These will be used for describing the general atmospheric circulation as a function of the seasons and time of the day (Table 1). The processed images will be used as input to the KAMM model. The methodology was presented in preliminary form at a satellite workshop (Hasager 1999).

	J	F	M	A	M	J	J	A	S	O	N	D
10:30		+	+			+		+/*	+		+	*
18:00		+	+			+		+	+			

Table 1. ERS-2 ATSR scenes for the Gulf of Suez (+) and Nile Valley (*) shown per month and time of the day.

The scenes are selected in order to capture the seasons with maximum and minimum winds, i.e. June and August/September with high winds and November/December and February with low winds. Also will the daily cycle of winds be analysed. The scenes from March and September are analysed to describe typical atmospheric conditions at the times of peak bird migrations. All available near-cloud free ERS-2 ATSR scenes received in the time interval 01-07-96 to 31-08-97 covering the Suez area are listed in Appendix A.

One ATSR scene maps a 500 km * 500 km area. Egypt covers 1000 km * 1000 km.

To map Egypt 9 ATSR scenes are used in a 10-day mosaic. Fig. 1 shows the approximate location of the 9 scenes. Minor parts of Egypt are not covered in this mapping.

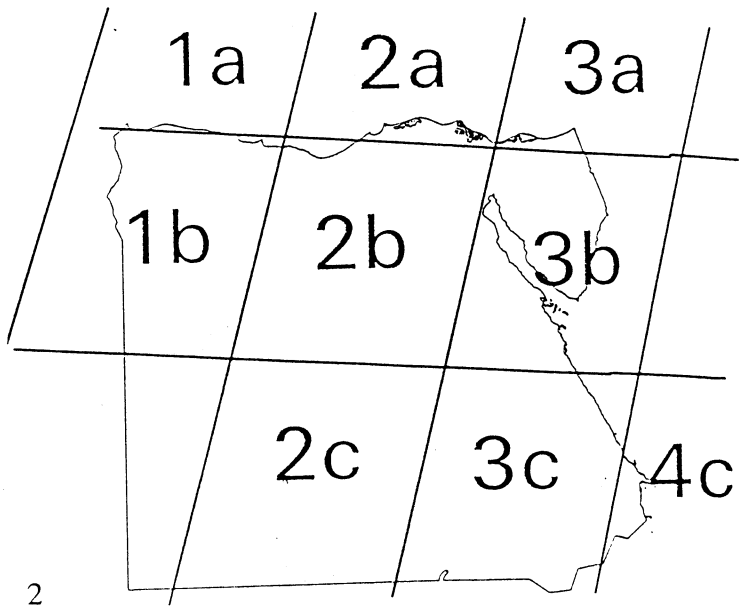

Fig. 1 Location of 9 ATSR scenes used for a mosaic map of Egypt. The scenes 1a and 1b are from 11-8-97; 2a, 2b and 2c from 2-8-97; 3a, 3b and 3c from 12-8-97 and 4c from 3-8-97 all in the morning.

ATSR was designed to provide

1) sea surface temperatures with absolute accuracy of better than 0.5°K with a spatial resolution of 50 km and in conditions of up to 80% cloud cover

2) images of surface temperature with 1 km resolution and 500 km swath, relative accuracy around 0.1°K.

These specifications are met (see reference "www 1"). It is data of the 1 km resolution that is retrieved and analysed in the current project. In daytime ERS-2 ATSR also records the reflected energy in bands centered around 1.6 μm (infrared reflectance), 0.87 μm (near-infrared reflectance), 0.67 μm (red reflectance) and 0.55 μm (green reflectance). See Appendix B for further details.

The scenes are geometrically rectified into latitude and longitude based on Clarke 1866 spheroid. The rectification algorithm is 2.order polynomial with bilinear convolution. The pixel size is approximately x=0.01097, y=0.01097 decimal degrees. The scenes are geolocated image to image (to a NOAA AVHRR satellite scene shown in Mortensen and Said (1996) and Hasager (1998)) and/or image to map (Digital Chart of the World vector layers (reference "www 2")). Further details are given in Appendix C.

Temperature results in Gulf of Suez from ATSR scenes

Evening temperatures

The evening scenes from the Gulf of Suez are shown in Figs. 2-6. A brief description of the land and sea surface temperature patterns are given below. In all evening scenes the land surfaces are cooler than the sea generally. It is very pronounced in winter.

In winter in February (Fig. 2) the maximum temperatures (18.7°C) are found in the Red Sea and in the Gulf of Aqaba. The temperatures in the Gulf of Suez decreases from south towards north (from 16.1 to 8.4°C). Land surfaces are even cooler and in mountains frost is found (-9,5°C) such as in Sinai and the mountain ranges east of Sahra esh Sharqiya. Temperatures in the Nile Valley are above freezing (~3.3°C).

In March (Fig. 3) frost is still found in the high mountains. The Gulf of Suez temperatures again decreases from south to north (from 16.1 to 11.1°C). The coast of Suez is cooler (5.8 to 8.4°C). The Nile delta and valley is warmer (8.4°C) than the desert around (5.8°C). Lake Birket Qârûn is warm (16.1°C) as is the city of Cairo (13.5-16.1°C). In the Mediterranean sea spots of clouds are seen (very cool).

Summer conditions in June (Fig. 4) and August (Fig. 5) show that the Red Sea has the same temperature at both times (23.8°C). The Gulf of Suez is warmer in August (23.8°C) than in June (21.2°C). Land surfaces are mainly cooler (18.7 to 21.1°C) than the sea. However in long stretches along the Gulf of Aqaba very warm land (28.9°C) is found. The western banks

of the Gulf of Suez has the same temperature as the sea. Hence no clear indication of coastline is seen. The coolest areas are in the northern desert at the Sinai Peninsula in June (11.0°C) and August (13.6°C).

The September evening temperature map (Fig. 6) shows very large gradients (from 8.4 to 31.5°C). The Gulf of Suez is at 23.8°C and the sourrounding land at 21.2°C. The Sinai is cooler (13.6 to 16.1°C). In the southern part of the scene very warm (23.8 to 31.5°C) land surfaces are found.

Evening scenes are recorded around 20:00 UTC, i.e. 22:00 local time. It means circa 4 hours after sunset. During the night the surfaces cool of to even lower temperatures. Land surfaces experience the largest changes due to their thermal properties. The heat capacity of water is much larger than that of e.g. sand. Further will turbulent mixing of the water reduce surface water cooling.

Morning temperatures

Morning temperature maps of the Gulf of Suez area from six months are given in Fig. 7-12. All morning maps show the sea surface to be cooler than the land surface. This is in contrast to all evening temperature maps (Fig. 2-6). The morning scenes are recorded around 8:00 UTC, i.e. 10:00 local time.

The February map (Fig. 7) shows the water temperatures of Gulf of Suez to increase from north to south (11.0 to 18.7°C). The Red Sea is even warmer (21.2°C) whereas the Mediterranean sea is cool (5.9-11.0°C). The coasts of Suez are very warm (23.8-28.9°C). The coolest land surface is in the heights of Sinai (Gebel Kathrîna, 5.9°C). The Nile delta and valley is significantly cooler (18.7°C) than the sourrounding deserts (23.8 to 28.9°C).

The March temperature map (Fig. 8) shows temperatures below zero. This effect is due to cloud cover (and further image processing will be done to make a cloud mask). Spatial temperature structures generally resembles those in the February temperature map (Fig. 7).

In June the land surface temperatures (Fig. 9) exceed the upper response of the ATSR scanner (~45°C). Therefore major areas are not really mapped (should be block out in black). The land surface is very warm (above 40°C). Only the Nile valley and delta is relatively cool (28.9 to 36.6°C) due to transpiration/evapotranspiration. The water of Gulf of Suez is cool decreasing from south towards north (from 34.0 to 21.2°C).

Later in the summer in August the land surface temperatures are lower than in June (compare Fig. 9 and 10). However the sea of Gulf of Suez is approximately at the same temperature in August as in June.

In September (Fig. 11) the land surface temperatures are further decreased. The western coast at the Gulf of Suez cools much down (from 41.7 to 31.5°C) within a month. The seas of Gulf of Suez and the Red Sea cools only little (from 23.8/34.0 to 23.8/31.5°C) with the North/South temperature gradient still present.

In November (Fig. 12) clouds are present over Saudi Arabia (plan to make a cloud mask). The sea of Gulf of Suez has a gradient from north (18.7°C) to south (23.8°C). The land surfaces at the coast of Gulf of Suez is warmer (26.4 to 28.9°C) than the sea and again the desert is warmer than the Nile valley and delta.

Temperature results in Zafarana and Hurghada from ATSR scenes

At Zafarana and Hurghada meteorological observations are sampled from masts. The seasonal variation in morning and evening temperatures measured by the ATSR thermal bands (i.e. in mornings the 11μm band, in evenings the 3.6μm band) are graphed in Fig. 13 and 14. The geographical coordinates of the four sites in Zafarana and Hurghada are listed in Table 2.

	Zafarana		Hurghada	
	Land site	Sea site	Land site	Sea site
N latitude (dd)	29.10	29.11	27.30	27.32
E longitude(dd)	32.60	32.69	33.70	33.77

Table 2 Latitude and longitude in decimal degrees (dd) for the four points where sea surface and land surface temperatures are observed at ERS-2 ATSR scenes.

The Zafarana land surface temperatures (LST) are sligthly cooler those at Hurghada (Fig. 13). For Zafarana the seasonal variation is between minimum (26°C) in February and maximum (43°C) in June. Sea surface temperature (SST) variations are much smaller. For Zafarana the minimum (14°C) is in March and maximum (23°C) in June. In August an unexpectedly low temperature is observed in Zafarana. Further investigation is in need. The sea near the coast of Hurghada is slightly warmer than at Zafarana, however equal at both sea sites from September to November. The much smaller seasonal variation in SST's (Δ 9°C) compared to LST's (Δ17°C) are due to mixing of water, the thermal properties and evaporation.

The evening temperatures at Zafarana and Hurghada are shown in Fig. 14. The main differences are in winter where LST's (from 4 to 8°C) are smaller than SST's (from 13 to 16°C) at both sites. In summer SST and LST vary very little and range between 22 and 24°C. This temperature should be compared to the morning temperatures in Fig. 13. For LST the diurnal variation between 8.00 and 22.00 local time is large of the order of 20°C. For SST the variation is only a few degrees.

Albodo results in Zafarana from ATSR scenes

The seasonal variations in albedo at the Zafarana land site and sea in the Gulf of Suez is graphed in Fig. 15a. The coordinates of the sites are listed in Table 2. The reflected sunlight in the 0.65μm band (red) varies from a minimum (52%) in March to maximum (74%) in June at the land site. The reflectance in 0.55μm band (green) varies much less and is generally lower. For the water surface the reflectance is very low and not very variable. A Normalized

Difference Vegetation Index (NDVI) is calculated as (Red-Green)/(Red+Green). The values are shown in Fig. 15b. For water the value is near zero. For the land rather constant around 0.3. Albedo maps will be input in the KAMM model. An example of an albedo map in the red band from 22 June 1997 is given in Fig. 16. The lowest values (13-16%) are found at the sea surfaces. The Nile valley and delta has 25% and the brighter areas of desert and mountains ranges between 40 and 90%.

Mosaic map of Egypt from ATSR scenes

To map Egypt from ATSR scenes nine are ordered (one is missing at the point of writing). The mosaic map (Fig. 17) shows the 8 scenes and a vector layer from Digital Chart of the World of the political border/coastline of The Republic of Egypt. The map is a 10-day composite from 2nd to 12th August 1997.

The map is in false colour with RED: 11μm, GREEN: 1.7μm and BLUE: 0.55μm. This means that surfaces dominated with 1) red areas have high temperatures (and low reflectance in 1.7 and 0.55μm), 2) green areas have high reflectance in 1.7μm (and low temperatures and low reflectance in 0.55μm), 3) blue areas have high reflectance in 0.55μm (and low temperatures and low reflectance in 0.65μm). Further does 4) black/dark areas have low reflectance/radiation in all bands and 5) white areas have high reflectance/radiation in all bands.

What is visible in the false colour composite mosaic map is the Nile delta and valley and some structures due to geomorphology and geology in the land areas (Fig. 17). Thin cloud cover in the Mediterranean sea is visible. All water bodies show up as dark areas.

Summary

From the AO3 call of the European Space Agency 20 ERS-2 ATSR GBT scenes were granted free of charge for studies of temperatures and albedo in the Gulf of Suez and Egypt. The ATSR scenes are geometrically rectified into latitude and longitude.

Temperature maps from morning and evenings through all seasons are described for the Gulf of Suez area. Large temperature gradients are found both on time and spatial scale. Especially noteworthy are the changes between land and sea surface temperatures reversing twice a day during the whole year. Further is the trend of strong temperature gradients in the sea surface in the Gulf of Suez of importance.

Future

Future analysis is underway. The main items will be
1) produce albodo and temperature map for Egypt (when the missing scene arrives)
2) calibrate land surface temperatures and albodo with new coefficients (if necessary)
3) combine analysis of local meteorological data and ATSR results in the Gulf of Suez area
4) input the ATSR albedo and temperature maps in the KAMM model

Acknowledgements

Granted 20 ERS-2 ATSR GBT scenes within the ERS-AO3 (**A**nnouncement of **O**pportunity) call from the European Space Agencey (ESA).

References

Hasager, C.B. 1998, Land and sea surface temperatures in northeast Egypt from the NOAA satellite, *Meteorology*, No. 9, Scientific technical and social journals (in Egypt), 3rd year, July 1998, p 1 (in arab)

Hasager, C.B. 1999 On the use of ATSR satellite images for wind resource assessment. *In full papers of International Workshop on the Applications of the ERS Along Track Scanning Radiometer*, ESRIN, ESA, Frascati, Italy 23-25 June 1999 (abstract for poster)

Mortensen N.G. and U. Said Said 1996 *Wind Atlas for the Gulf of Suez*, Risø, Denmark, pp 115

www 1: http://earth1.esrin.esa.it/esa_doc/doc_ats.html (ERS ATSR documentation)

www 2: http://ortelius.maproom.psu.edu/dcw/ (Digital Chart of the World)

List of figures

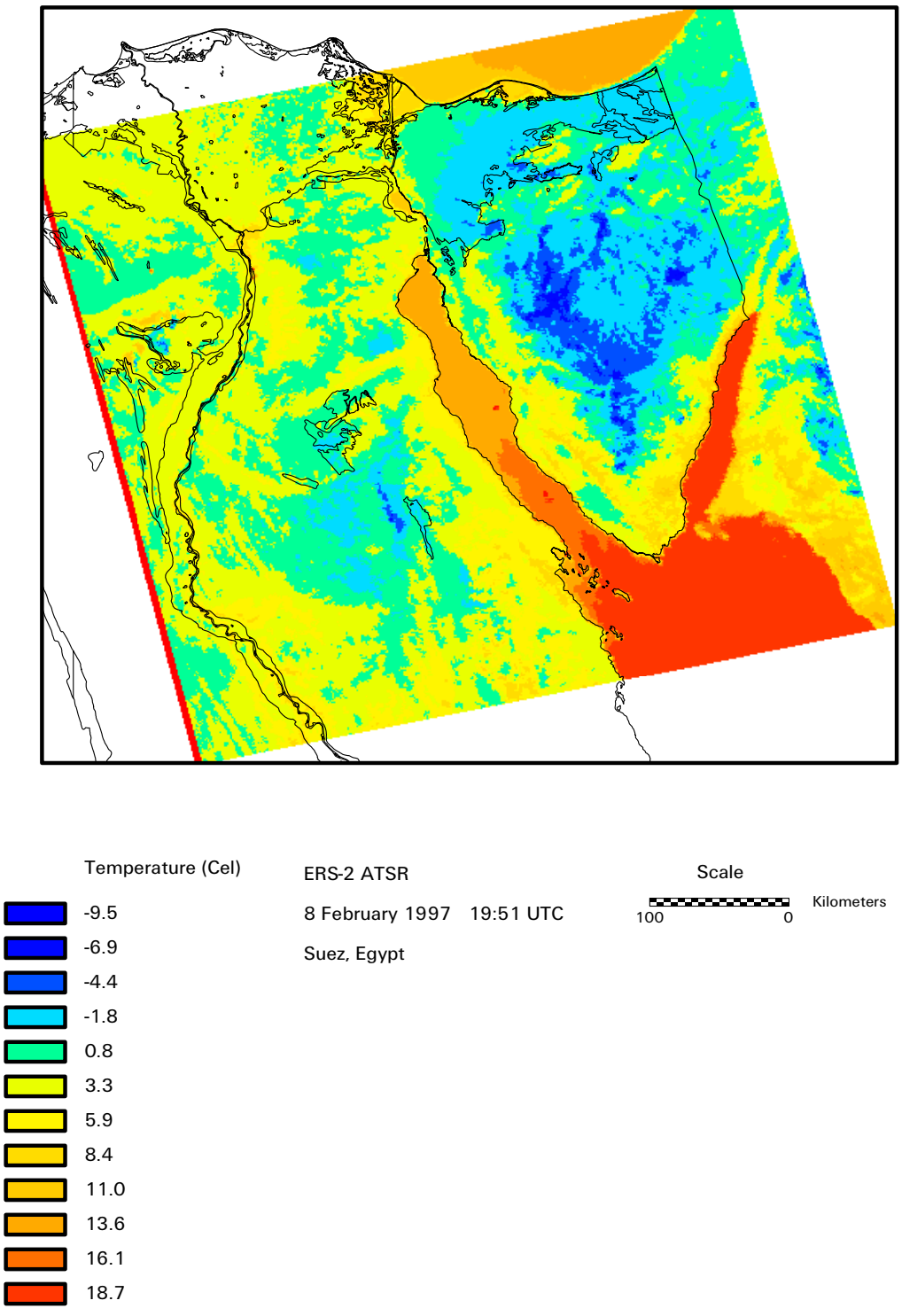

Fig. 2. Temperature [ºC] from ERS-2 ATSR, 8 February 1997 @ 19:51 UTC.

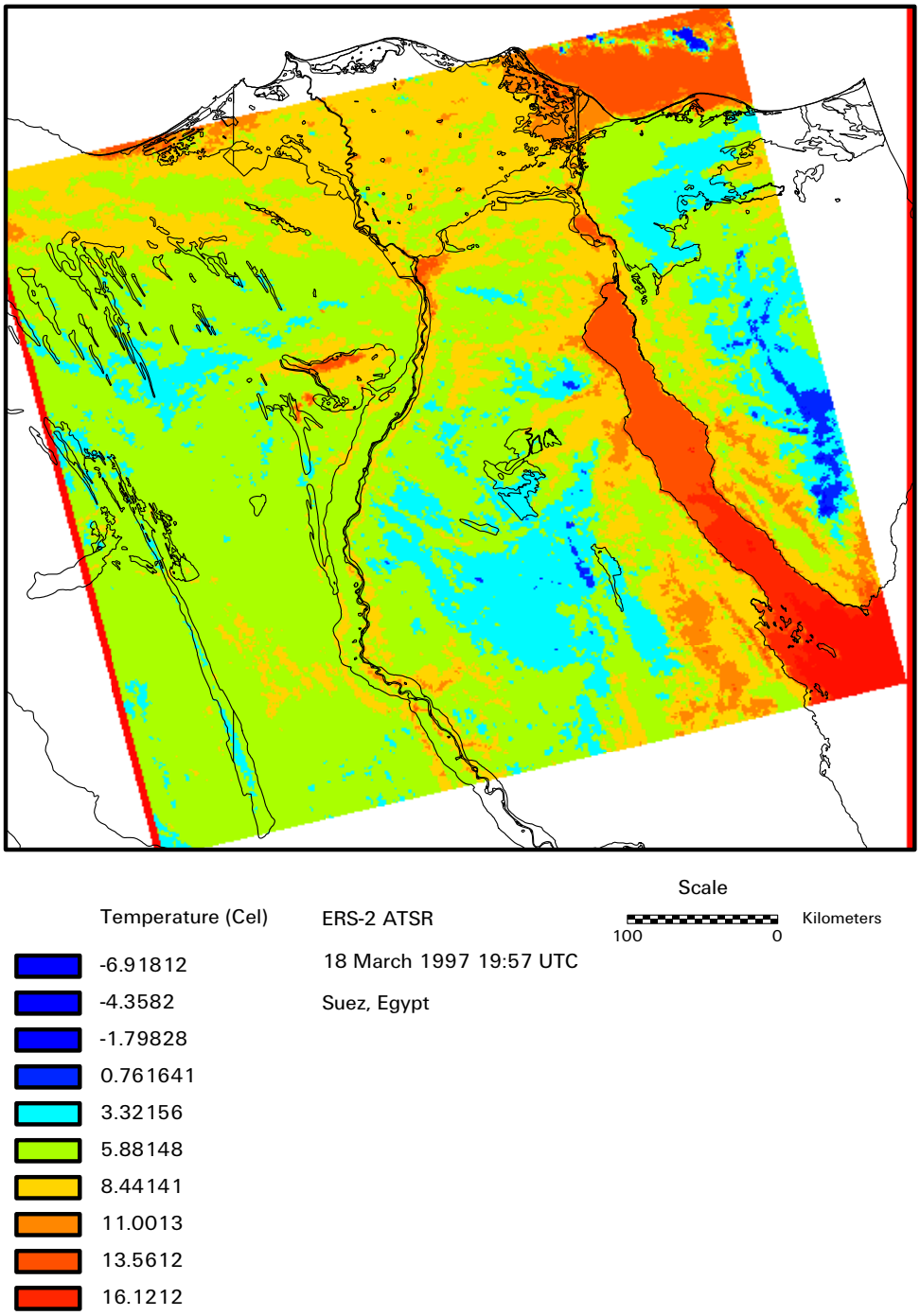

Fig. 3. Temperature [ºC] from ERS-2 ATSR, 18 March 1997 @ 19:57 UTC.

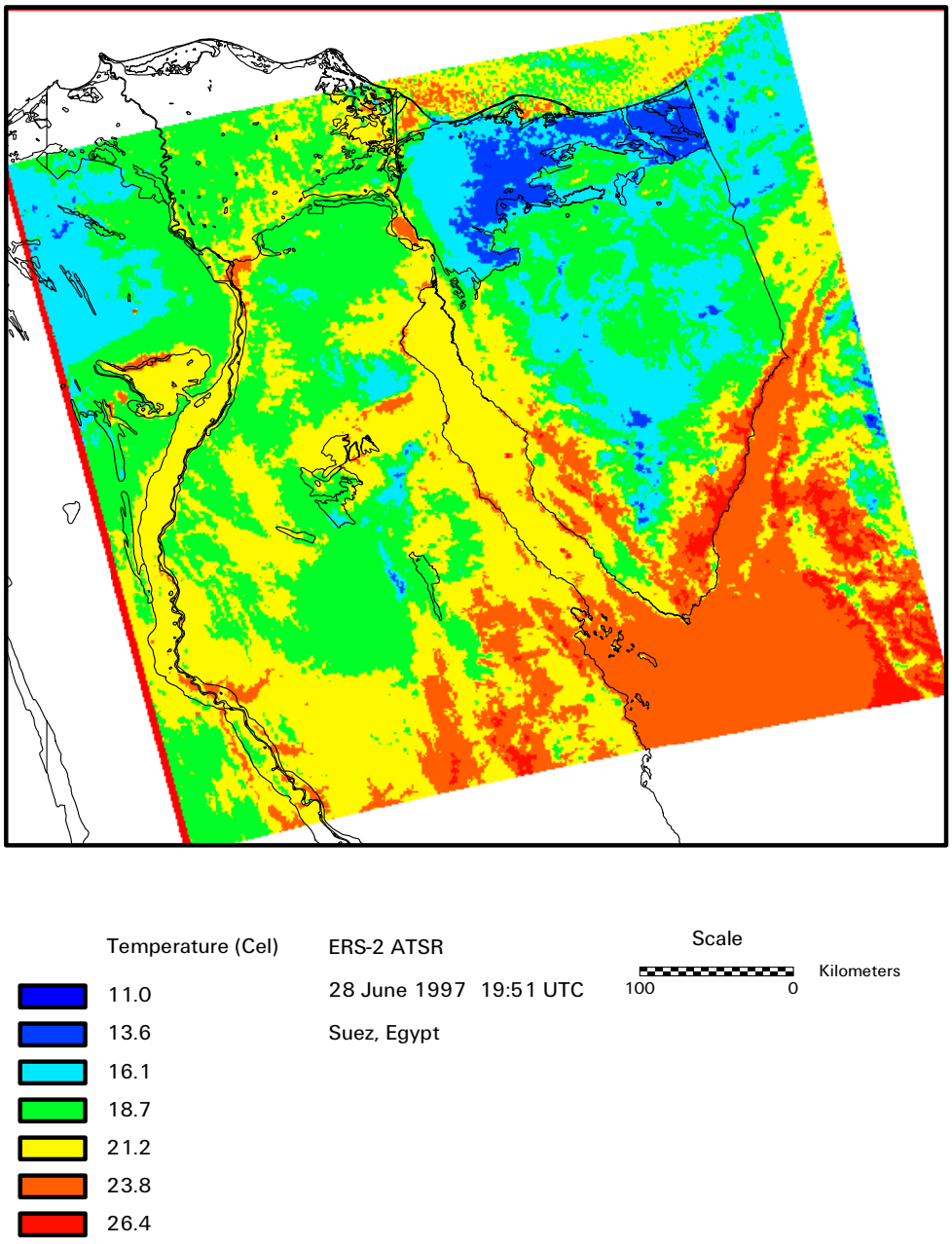

Fig. 4. Temperature [ºC] from ERS-2 ATSR, 28 June 1997 @ 19:51 UTC.

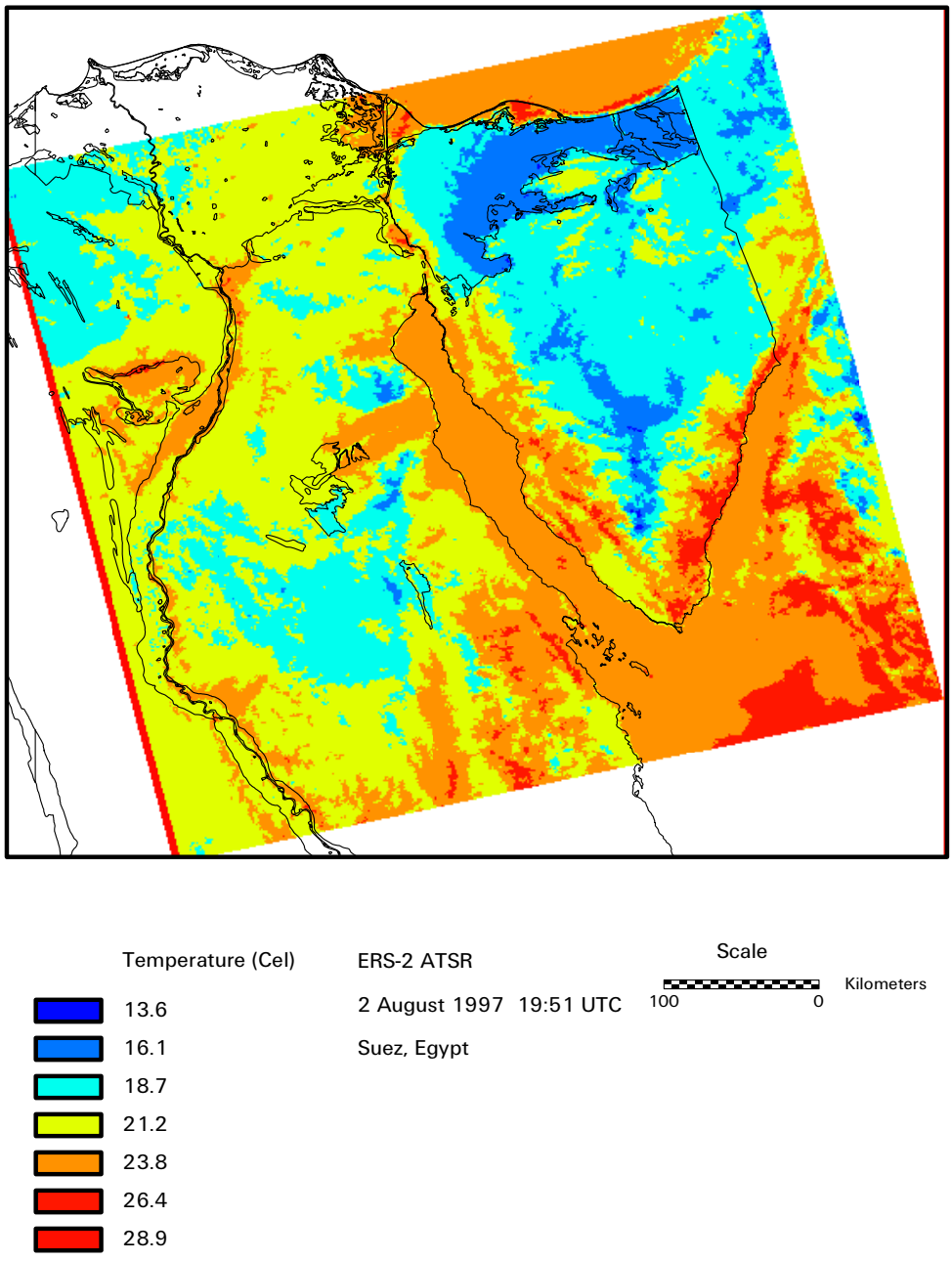

Fig. 5. Temperature [ºC] from ERS-2 ATSR, 2 August 1997 @ 19:51 UTC.

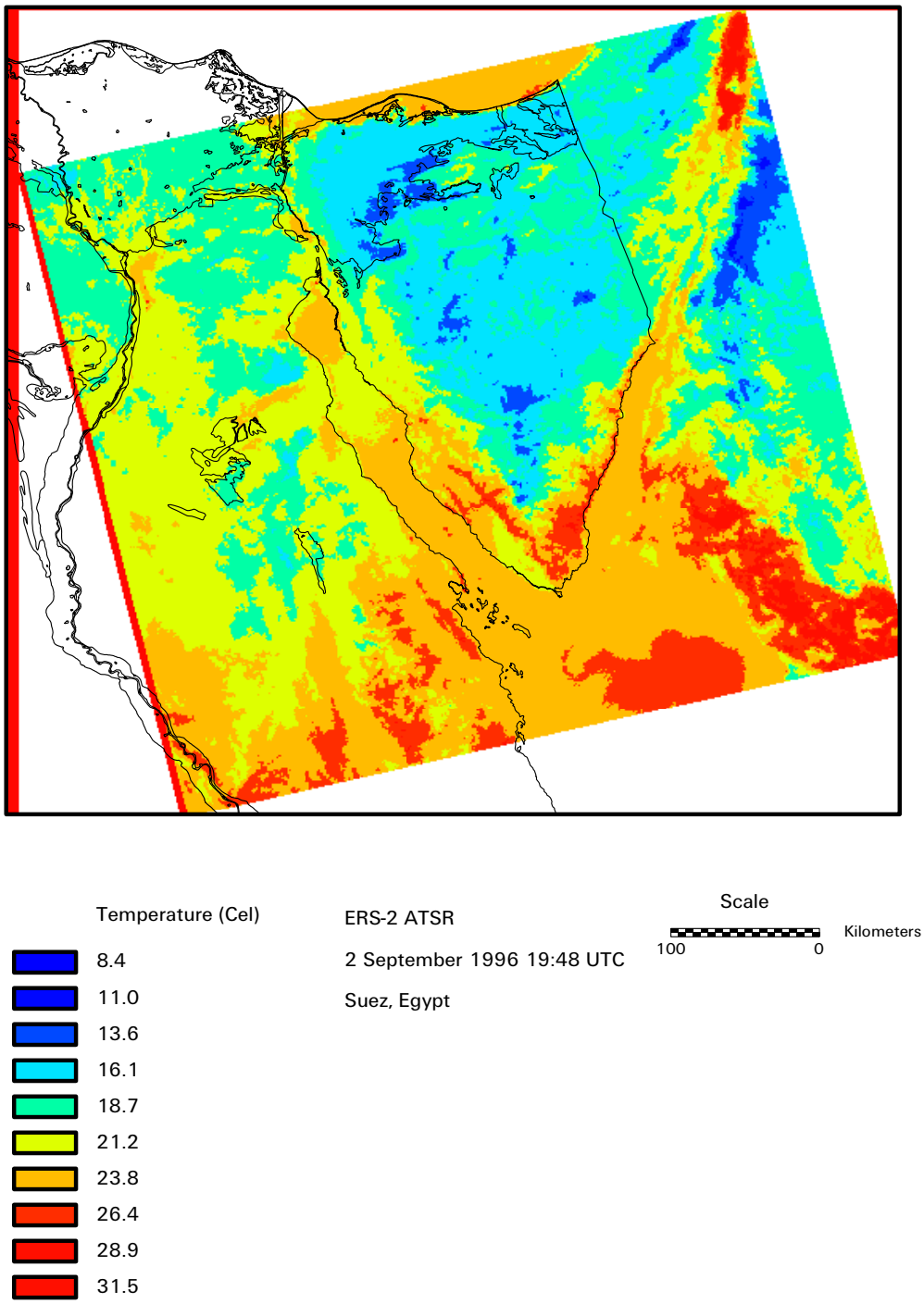

Fig. 6. Temperature [ºC] from ERS-2 ATSR, 2 September 1996 @ 19:51 UTC.

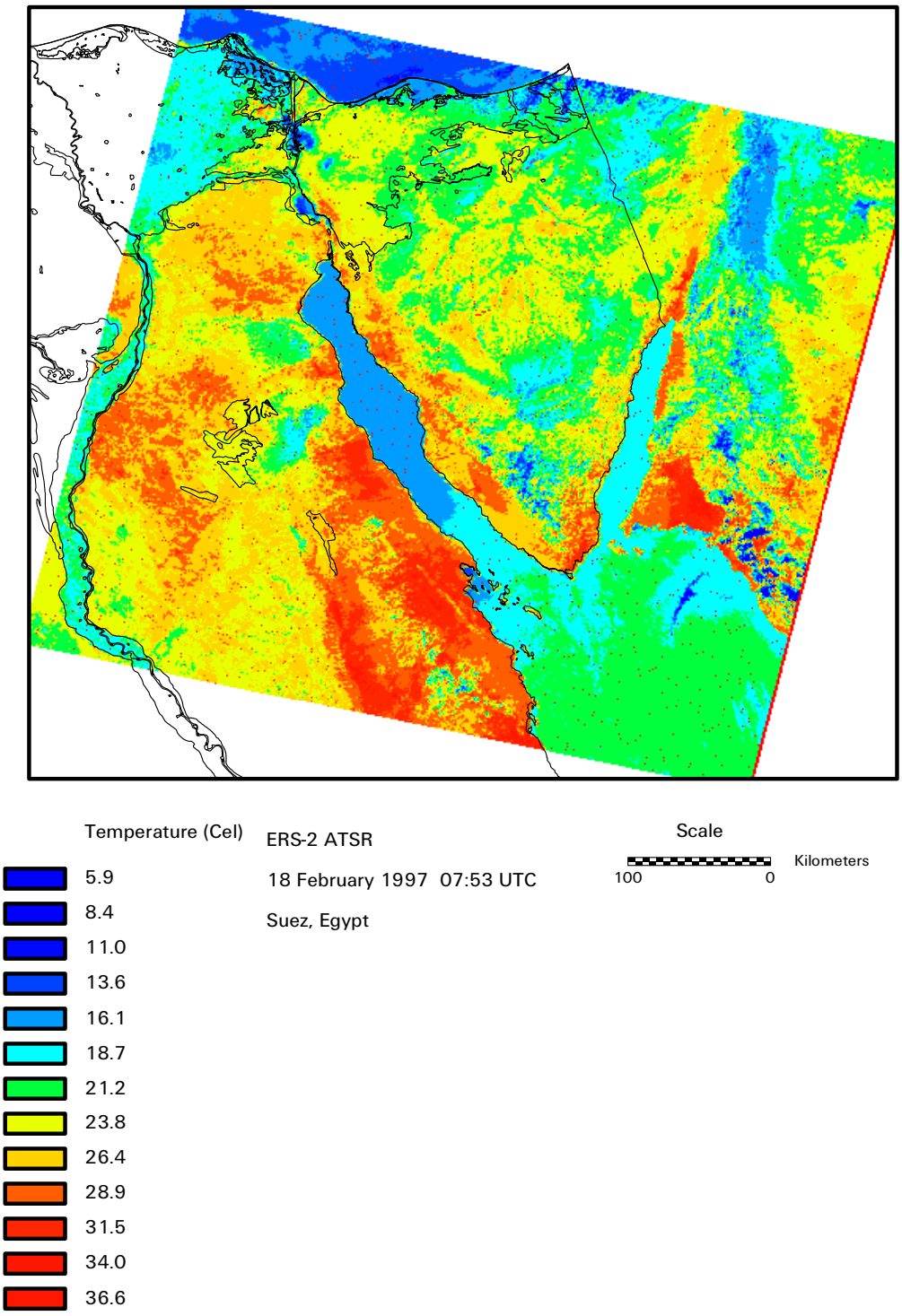

Fig. 7. Temperature [ºC] from ERS-2 ATSR, 18 February 1997 @ 07:53 UTC.

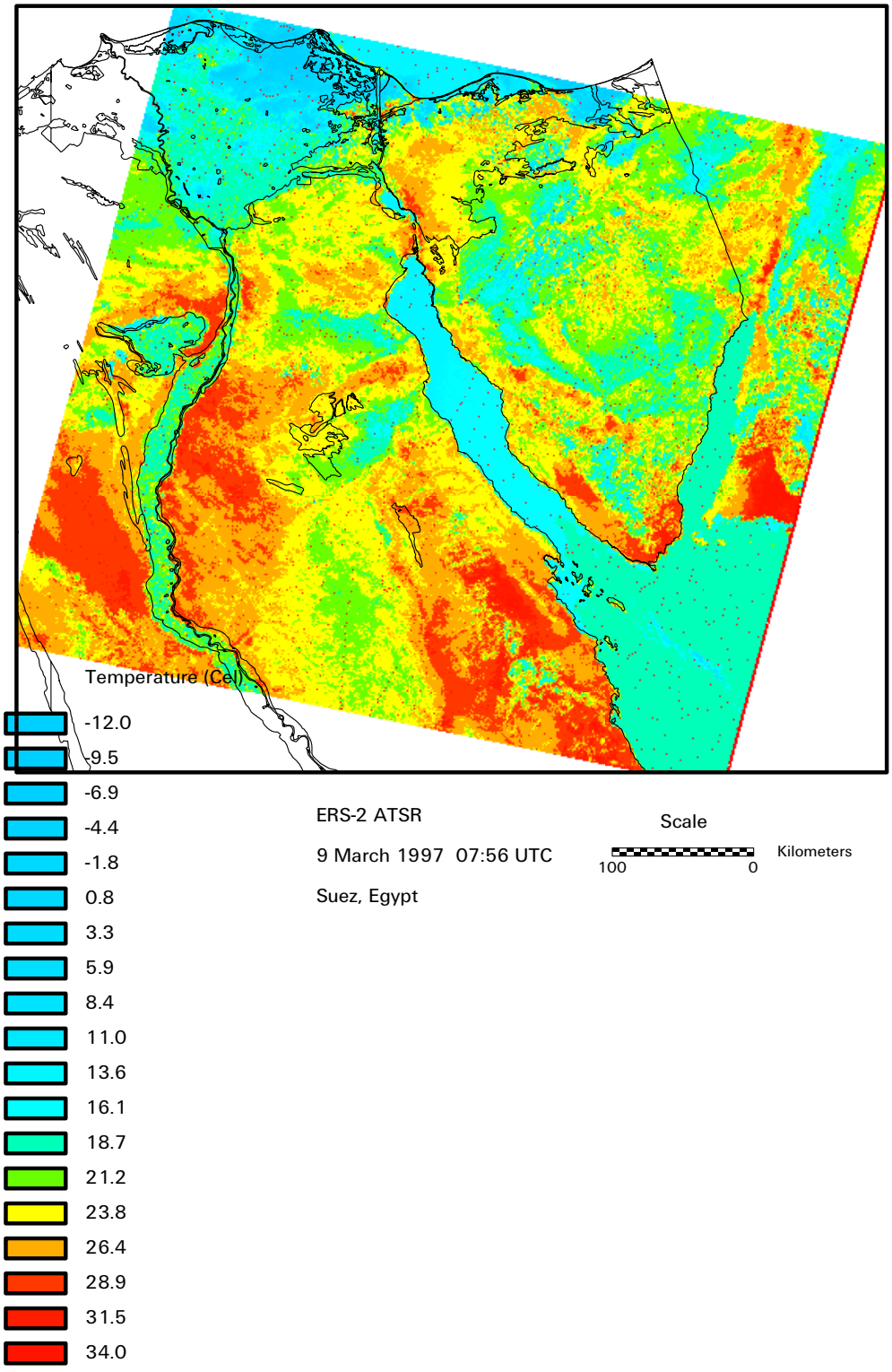

Fig. 8. Temperature [ºC] from ERS-2 ATSR, 9 March 1997 @ 07:56 UTC.

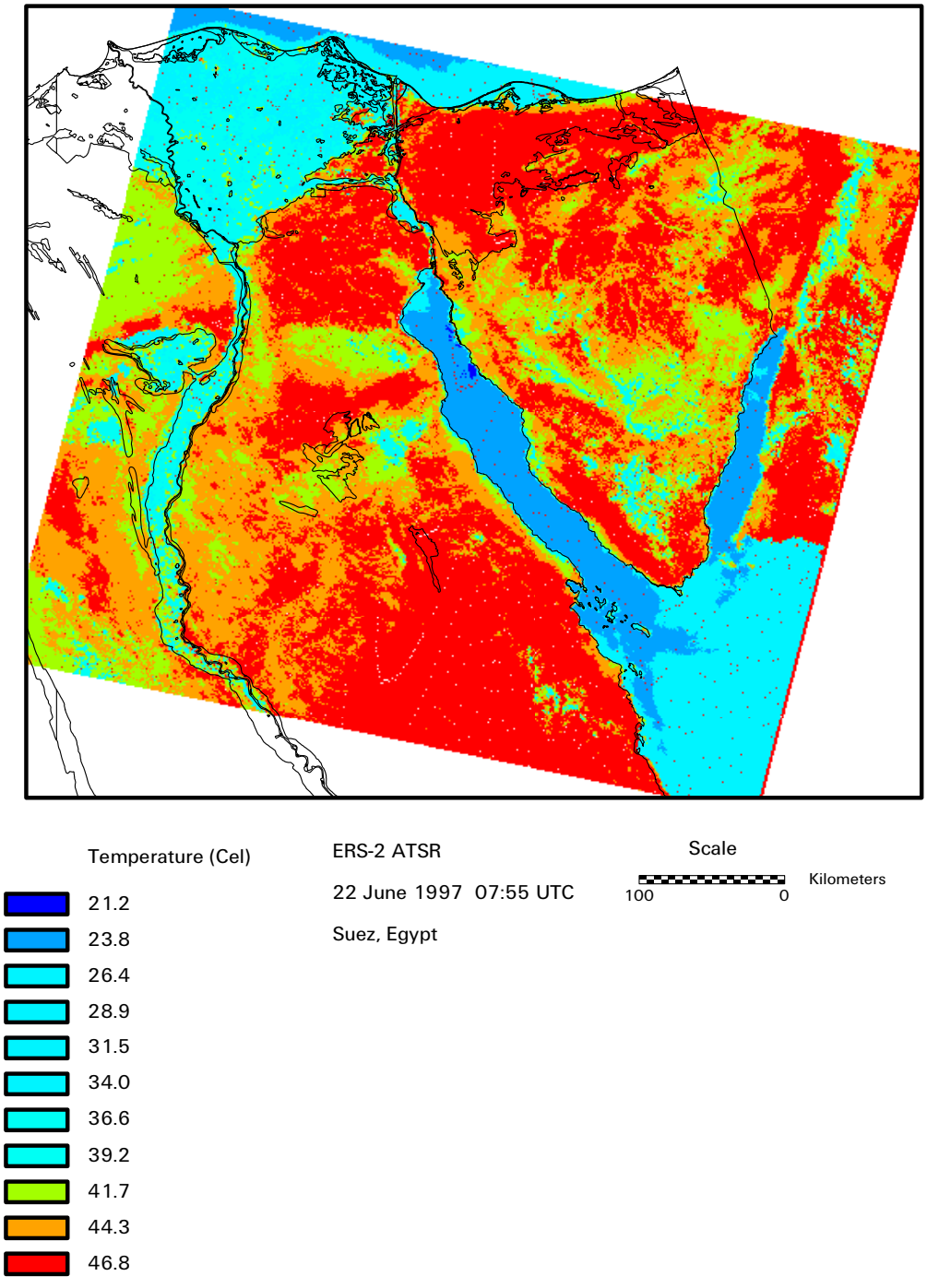

Fig. 9. Temperature [ºC] from ERS-2 ATSR, 22 June 1997 @ 07:55 UTC.

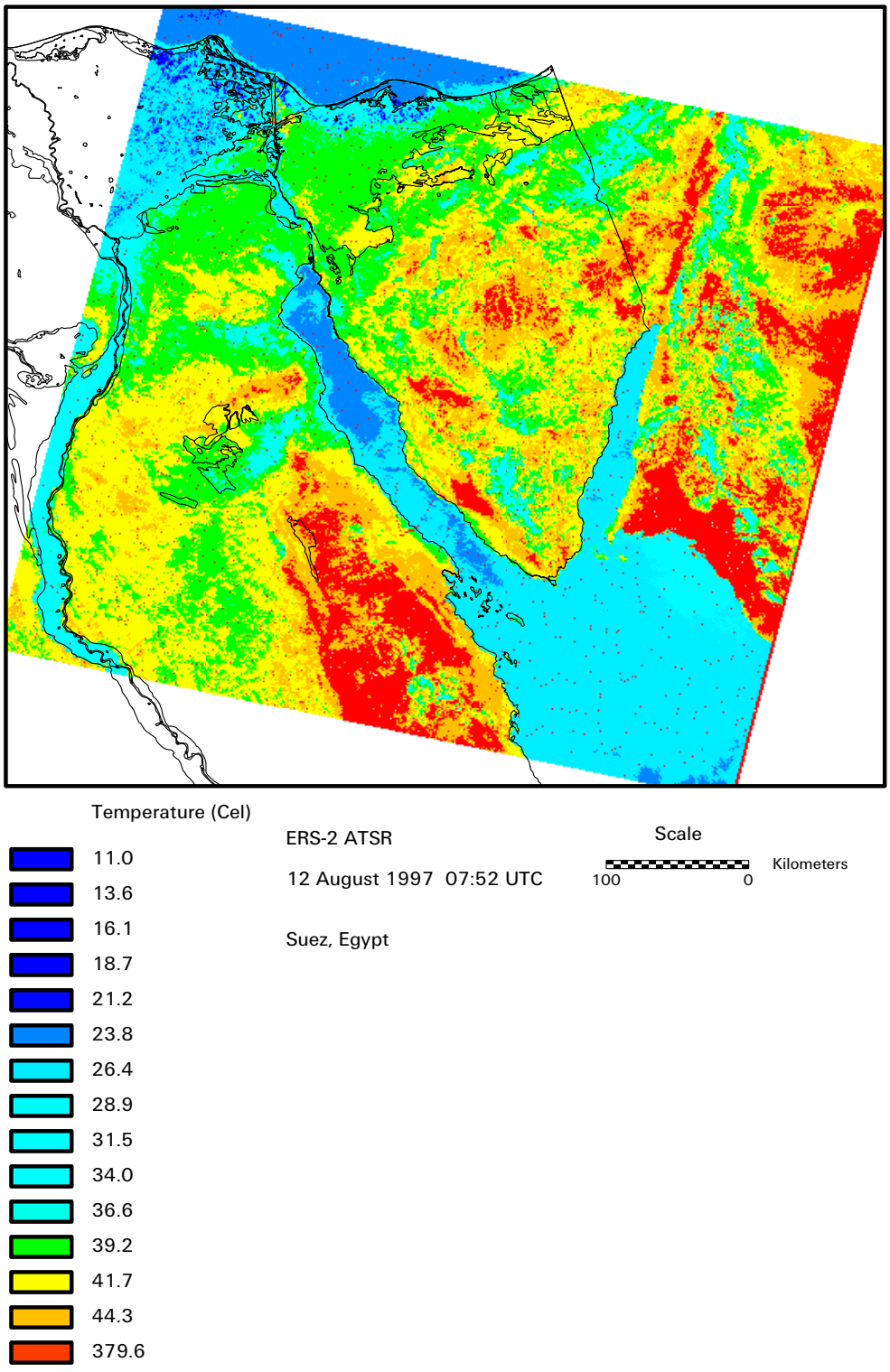

Fig. 10. Temperature [ºC] from ERS-2 ATSR, 12 August 1997 @ 07:52 UTC.

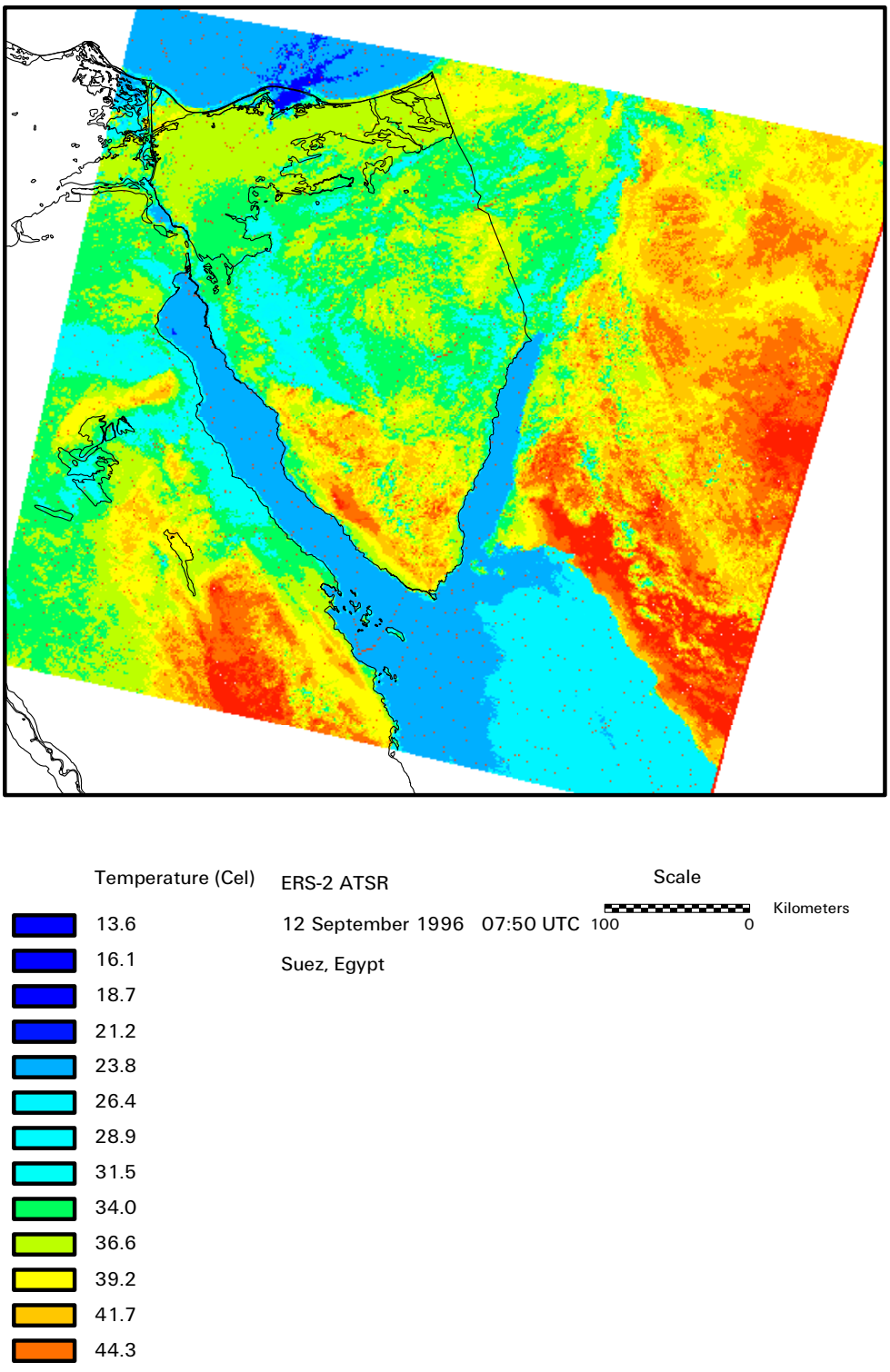

Fig. 11. Temperature [ºC] from ERS-2 ATSR, 12 September 1996 @ 07:50 UTC.

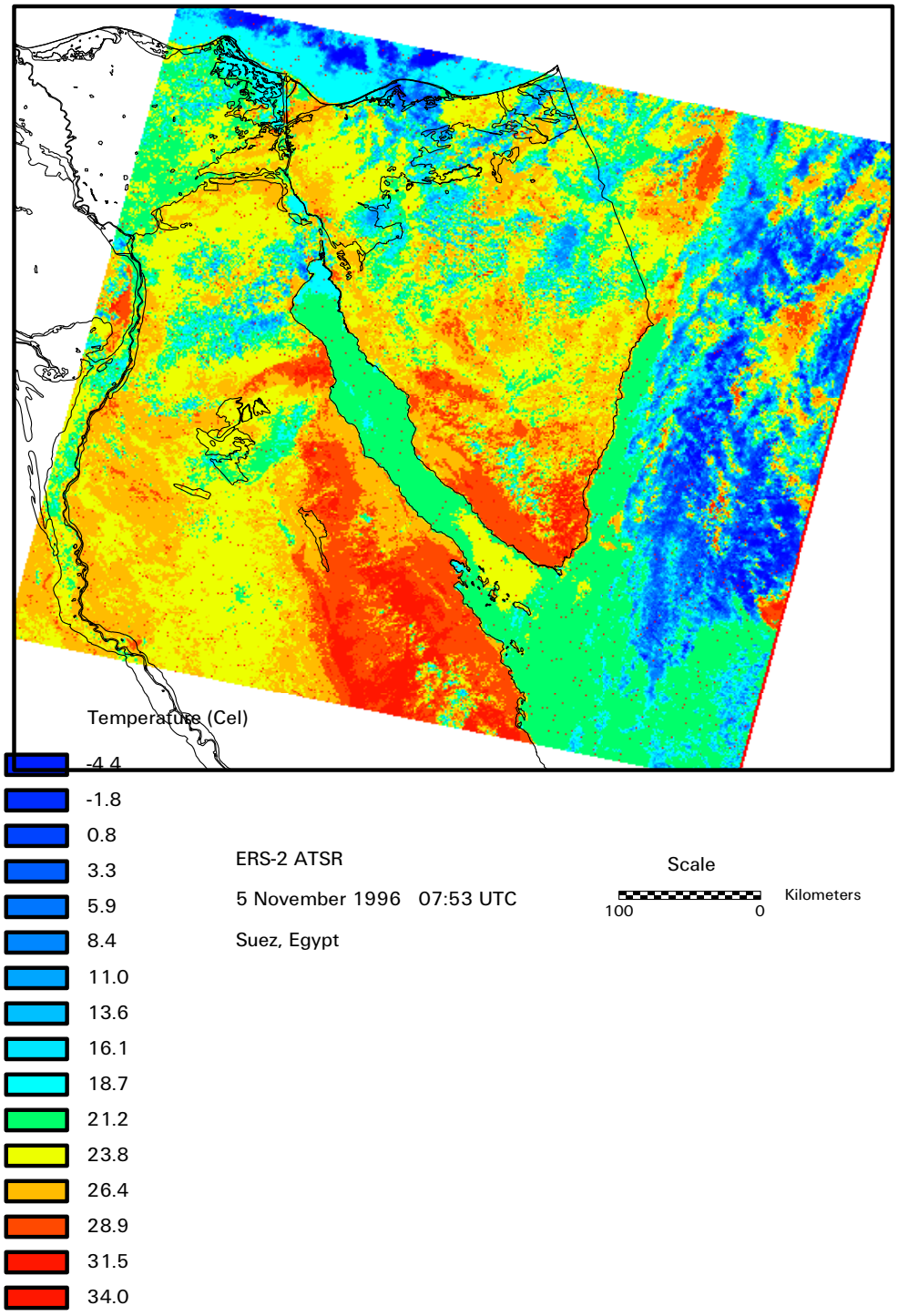

Fig. 12. Temperature [ºC] from ERS-2 ATSR, 5 November 1996 @ 07:53 UTC.

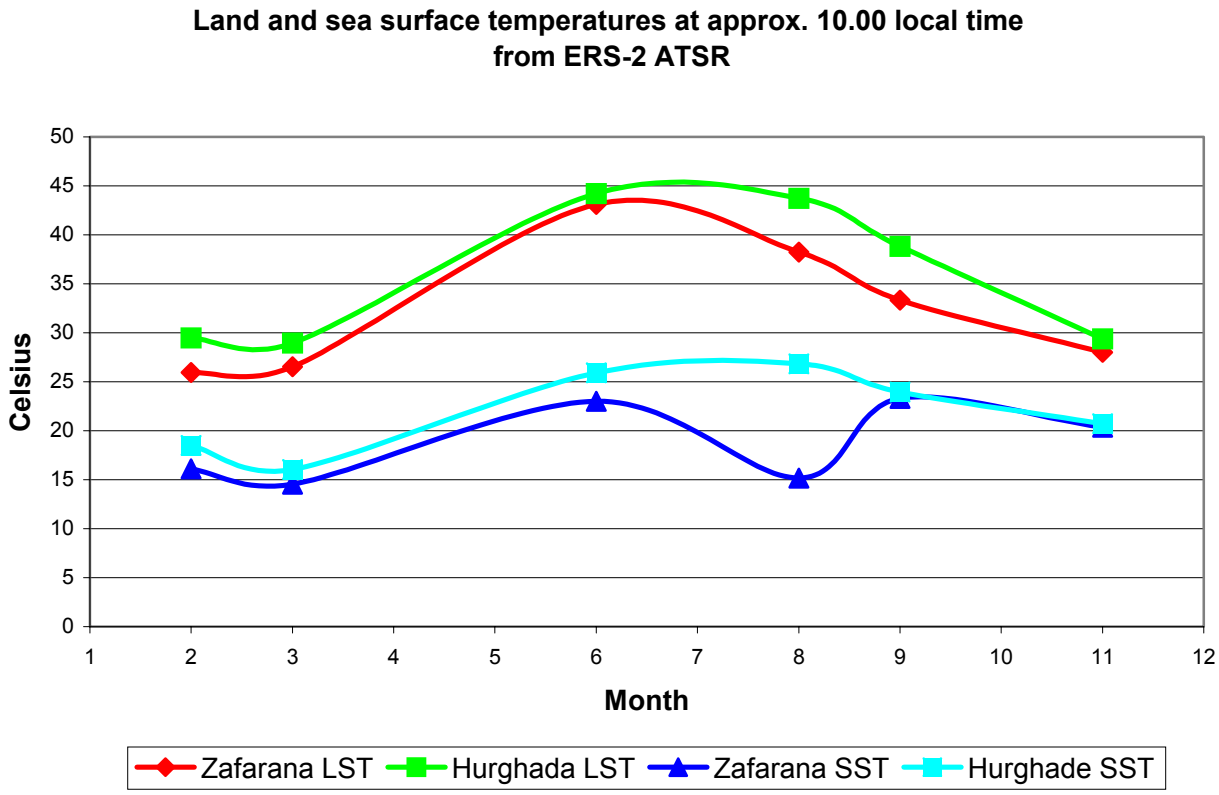

Fig. 13. Land and sea surface temperatures at approx. 10.00 local time from ERS-2 ATSR.

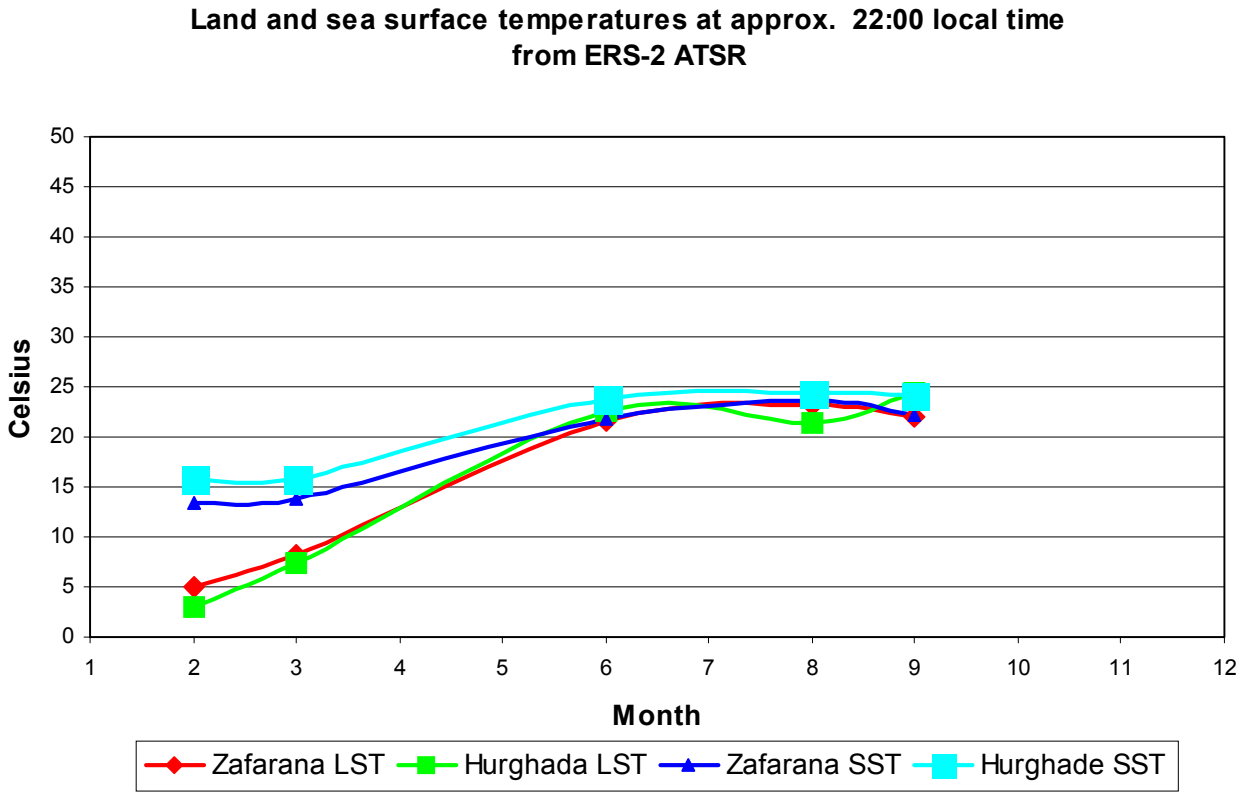

Fig. 14. Land and sea surface temperatures at approx. 22:00 local time from ERS-2 ATSR.

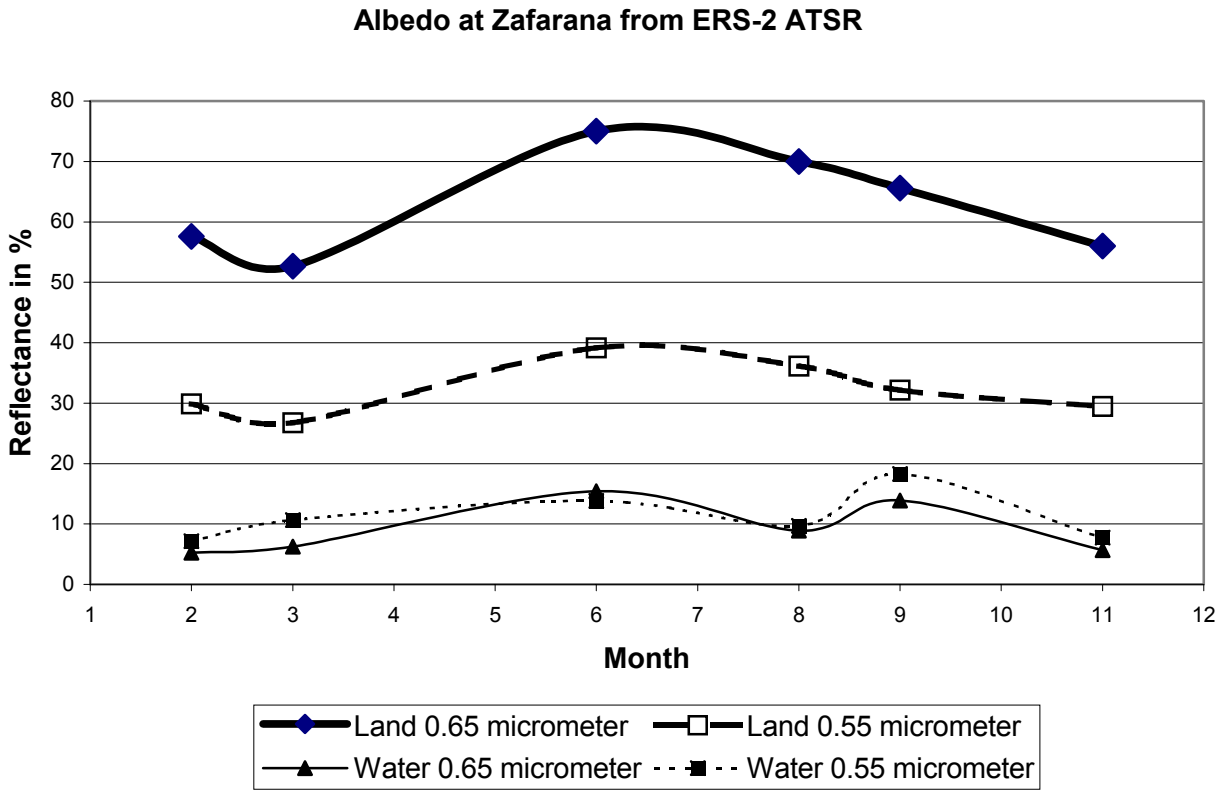

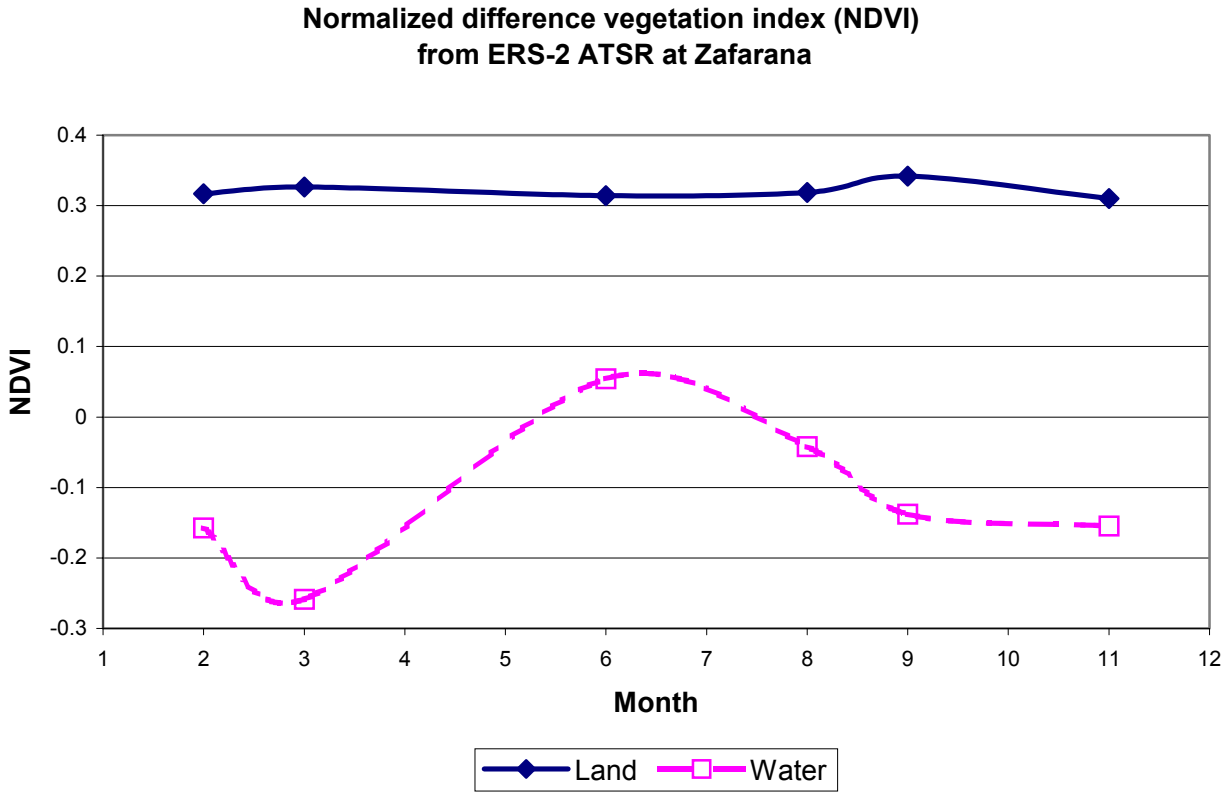

Fig. 15. A: Albedo at Zafarana from ERS-2 ATSR.
B: Normalized difference vegetation index (NDVI) from ERS-2 ATSR at Zafarana.

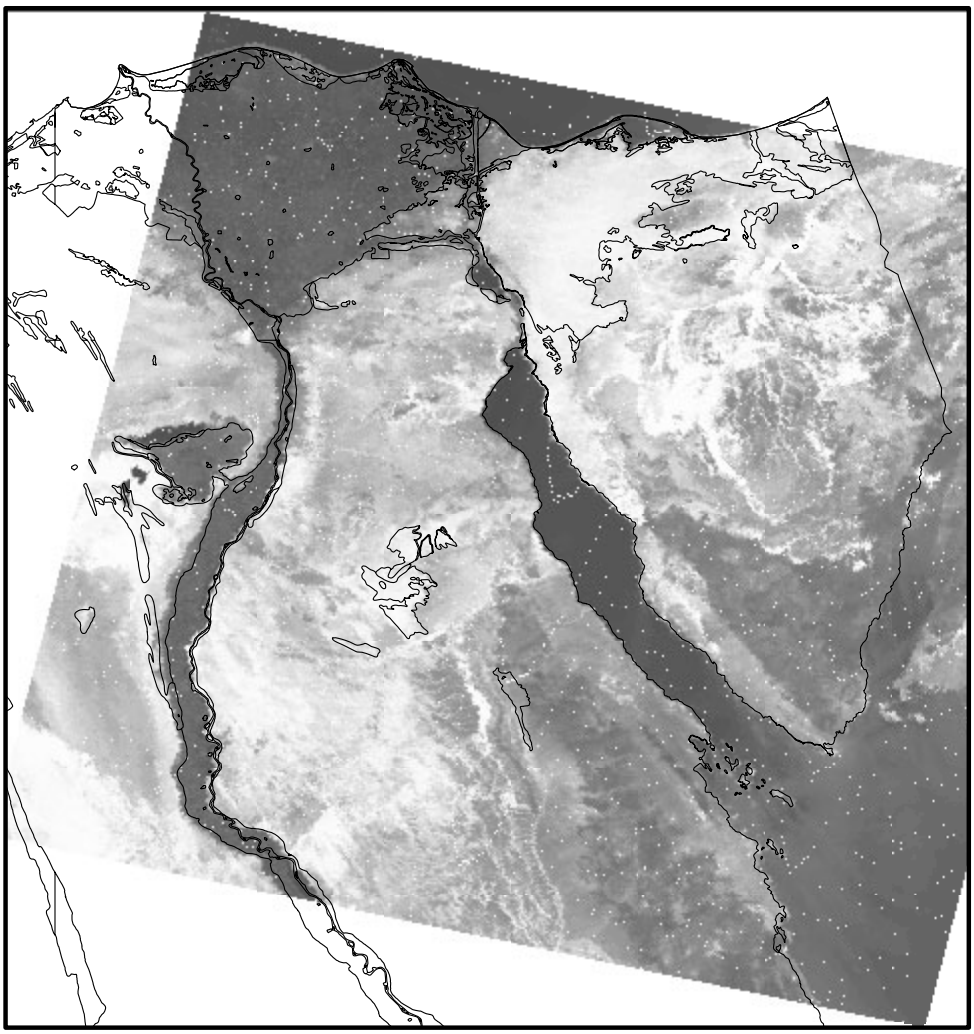

Fig. 16. ERS-2 ATSR, 22 June 1997 @ 07:55 UTC. Albedo of red channel (0.65 micrometer).

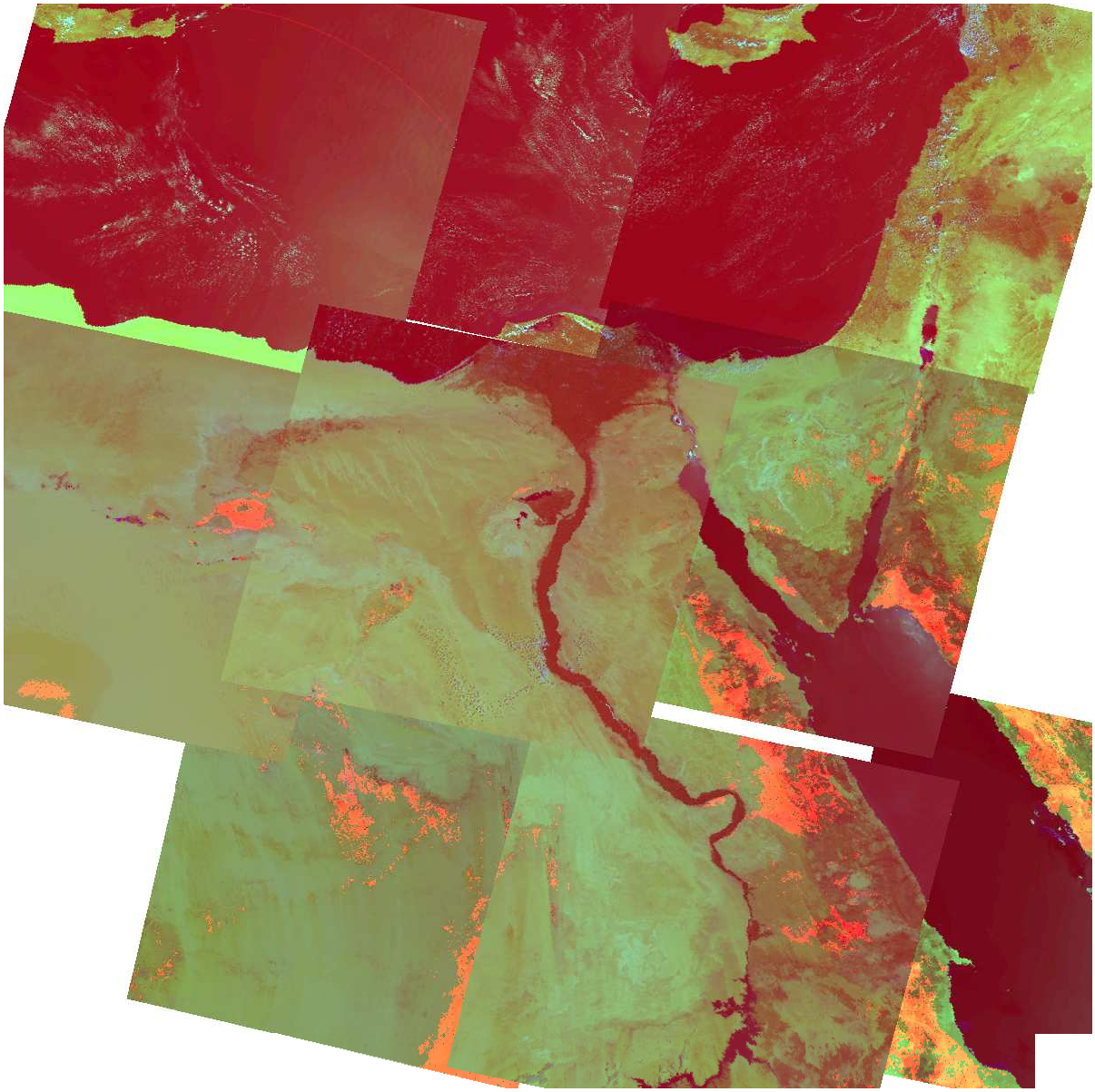

Appendix A

Available ERS-2 ATSR scenes

How to find out about available ERS ATSR scenes

At Internet it is possible to get fast and reliable information on the available ERS ATSR satellite scenes for a chosen location on earth.
The internet address is
http://earthnet.esrin.esa.it/reg/uag/cgi/product?FROM=catalogue
or go through http://earthnet.esrin.esa.it/
Cataloques, Multimissions query, Single mission, ERS-2 ATSR and give appropriate coordinates (e.g. Suez 29° N latitude and 33° E longitude).
Query outputs are ordered in frames, orbits, tracks or time (as desired) and shown both on an overview map and sometimes as quicklooks. Quicklooks are effective to show cloud-patterns. For daytime scenes the quicklook is in colour (false composite of several channels). For evening scenes the quicklook is in black & white (only the thermal channel is useful). Further is nominal geometrical coordinates given.

As the Gulf of Suez area is of main interest a listing of all available near-cloud free ERS-2 ATSR scenes in the time interval 01-07-1996 to 31-08-1997 are given in Table A1.

Approx 8:00 UTC frame 3015	Approx 20:00 UTC frame 0585
1997-08-12*	1997-08-15
1997-06-22	1997-08-05
1997-06-19	**1997-08-02**
1997-06-06	**1997-06-28**
1997-04-10	1997-06-25
1997-03-09	1997-06-09
1997-02-18	1997-05-08
1997-01-30	**1997-03-18**
1996-12-26	1997-02-27
1996-12-10	**1997-02-08**
1996-11-21	1997-02-05
1996-11-05	1997-01-07
1996-10-20	1997-01-04
1996-10-01	1996-12-19
1996-09-15	1996-10-23
1996-09-12	1996-10-07
1996-08-11	1996-09-18
1996-08-08	**1996-09-02**
1996-07-23	1996-08-17
1996-07-07	1996-08-14
	1996-08-01
	1996-07-13

*Table 2. All available (near) cloud free ERS-2 ATSR scenes from the Gulf of Suez area between 1 July 1996 and 31 August 1997. The scenes **in bold are the ones analyzed** in the current project .The scene marked with * is from the Nile river, not Gulf of Suez.*

Appendix B

Basic image processing

The ATSR scenes are processed at a VMS system and can be read in a c-programme please refer to
http://www.atsr.rl.ac.uk/html/obtaining.html
http://www.atsr.rl.ac.uk/source/c/get_sadist2_gbt.c
http://earth1.esrin.esa.it/esa_doc/doc_ats.html
The image data structure is described at the above sites.

To import the scenes into the ERDAS Imagine 8.3 ©(Registred trademark) image processing software (at a HP workstation) it is necessary to byte-swap the scenes. Raw image data are stored as unsigned 16 bytes. Record-length is 1024 and the image size 512*512. Further it is necessary to flip and/or rotate the raw scenes. Each scene has 14 bands, i.e. a nadir scan and a forward scan each with 7 bands. The seven spectral bands are centered at

12 μm (thermal radiation)
10.8 μm (thermal radiation) (often named the 11μm band)
3.7 μm (thermal radiation/middle infrared reflectance)
1.6 μm (infrared reflectance)
0.87 μm (near-infrared reflectance)
0.67 μm (red reflectance)
0.55 μm (green reflectance)

About the ATSR (Along-Track Scanning Radiometer) on-board ERS-2

ATSR scans with a field of view of the Earth's surface in two curved swaths, 500 km wide and 900 km apart (see figure). ATSR has a dual viewing of the same piece of Earth through the atmosphere at two different angles with a very short time interval (150 seconds) in-between the forward and nadir view. This feature makes it possible to correct for the atmospheric contribution on the remotely sensed electromagnetic signals. The result is precise sea surface temperature maps atmospheric corrected.

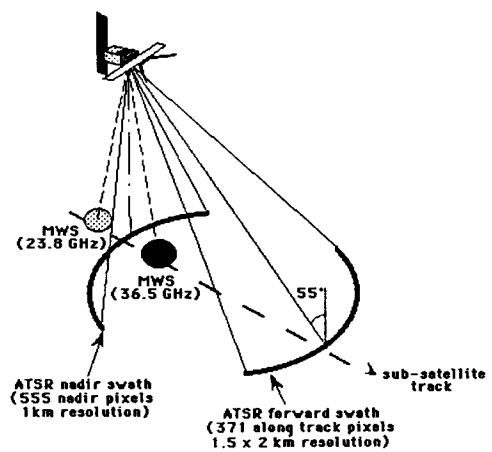

Figure B1 from http://earth1.esrin.esa.it/0xc1cce41c_0x000317fa

The scenes used in the current project are the so-called GBT (gridded brightness temperature) product. This means that the pixels from the forward and nadir pixles are collocated into a 512 * 512 grid of 1 km* 1 km pixels. The brightness temperatures and reflectances are calibrated.

Only channel 3.7μm is useful in the 5 evening scenes (i.e. band 9) and channels 11μm, 1.6μm, 0.65μm and 0.55μm (i.e. bands 2, 4, 6, 7, 11 (note 4 and 11 are the 1.6μm in nadir and forward, respectively) in the 15 morning scenes from Egypt.

Appendix C

Geometrical rectification

The geometrical rectification of ATSR scenes in the Gulf of Suez area are geolocated to a NOAA AVHRR scene (image to image) including some information from vector layers of the Digital Chart of the World (DCW).

The NOAA AVHRR scene was geometrically corrected image to map based on 15 locations found in the map 1:1.000.000 from John Bartholmew and Son LTD MCMLXXVIII of "Egypt". A second-order polynomial with resulting root means square error 0.7. In the desert areas no pixels were easily recognized, so these areas will in general tend to have larger errors. The NOAA AVHRR scene is presented in Mortensen and Said (1996, p 64-66) and Hasager (1998).

In areas outside the Gulf of Suez only the Digital Chart of the World ("www ref 2") vector layers have been available. The vector layers used are political/ocean lines (ponet) of Egypt, Libya, Israel, Lebanon, Syria, Saudi Arabia, Cyprus and Greece). Further from Egypt are included information on drainage (dnnet), hypsography (hynet), land cover (lcpoly), physiography (phline), railroads (rrline) and utilities (utline). Other available layers from DCW include populated places, ocean features, aeronautical and cultural landmarks. These layers were not used, however. To get the Digital Chart of the World free of cost, please refer to http://ortelius.maproom.psu.edu/dcw/

The geometrical rectification is based on approximately 20 ground control points (GCP) in each scene and the root mean square errors for x, y and total are reported in Table C1. Please note that the best rectification is in Suez morning scenes. GCP's are more difficult to identify at night (only 3.7μm band is available). For the Egypt mosaic very few GCP could be found (~10) and a 1.order transform seemed to give better results than a 2.order in some cases.

date	time UTC	frame	orbit	track	GCP	rms_x	rms_y	rms	mosaic
Suez morning scenes									
1997-08-12	07:52:58	3015	12085	00207	27	1.4	2.4	2.8	3b
1997-06-22	07:55:51	3015	11355	00479	25	2.1	2.3	3.1	
1997-03-09	07:55:48	3015	09852	00479	20	1.8	1.7	2.5	
1997-02-18	07:52:54	3015	09580	00207	19	2.6	2.1	3.3	
1996-11-05	07:52:59	3015	08077	00207	18	2.3	1.4	2.6	
1996-09-12	07:50:07	3015	07304	00436	18	1.7	0.7	1.6	
Suez evening scenes									
1997-08-02	19:51:31	0585	11949	00071	20	2.0	2.4	3.2	
1997-06-28	19:51:32	0585	11448	00071	24	4.2	1.6	4.5	
1997-03-18	19:57:14	0585	09988	00114	24	1.9	6.0	6.3	
1997-02-08	19:51:27	0585	09444	00071	23	5.4	2.8	6.0	
1996-09-02	19:48:40	0585	07168	00300	9	3.6	5.7	6.7	
Nile									
1996-12-10	07:52:53	3105	08578	00207	19	3.3	2.5	4.2	
Egypt mosaic									
western row (near Libya)									
1997-08-11	08:24:35	2925	12071	00193	9	2.4	1.9	3.0	1a
1997-08-11	08:24:35	3015	12071	00193	7	3.5	1.9	4.0	1b
middle row (Egypt desert area)									
1997-08-02	08:07:20	2925	11942	00064	8	1.6	1.7	2.3	2a
Missing at the moment									
1997-08-02	08:07:20	3105	11942	00064	16	4.9	7.9	8.6	2c
middle row (Suez/Nile area)									
1997-08-12	07:52:58	2925	12085	00207	12	4.1	5.2	6.6	3a
1997-08-12	07:52:58	3015	12085	00207	27	1.4	2.4	2.8	3b
1997-08-12	07:52:58	3105	12085	00207	12	1.8	5.6	5.9	3c
eastern row (Red Sea area)									
1997-08-03	07:35:43	3105	11956	00078	12	1.5	2.0	2.5	4c

Table C1 Listing of 20 analyzed ATSR scenes with date, time (start of recording in UTC read in header lines af raw data), frame, orbit, track, number of ground control points (GCP), root mean square errors for x, y and total. The mosaic map numbering from Fig. 1.

Bibliographic Data Sheet **Risø-I-1969(EN)**

Title and authors

Wind Atlas for the Gulf of Suez: Satellite Imagery and Analyses

Charlotte B. Hasager

Department or group	Date
Wind Energy Department	April 2003

Groups own reg. number(s)	Project/contract No(s)
VES 1170 104-00 MET 1105 104-00	Danida 1305/473 (104.Egypten.32)

Sponsorship

Danish Ministry of Foreign Affairs (Danida)

Pages	Tables	Illustrations	References
46	7	32	7

Abstract (max. 2000 characters)

Satellite imagery and data have been used to investigate the spatial distributions of wind speed and some terrain surface characteristics in the Gulf of Suez. The methods and the results are described in three separate sections:

1. "Comparing SAR winds and in-situ winds". Synthetic Aperture Radar (SAR) data derived from the European Remote Sensing Satellite (ERS) have been used to make wind speed maps for the Gulf of Suez.
2. "Land cover from Landsat TM imagery". Landsat Thematic Mapper (TM) data have been used to establish true- and false-colour land cover maps, as well as land cover classification maps.
3. "Reporting on satellite information for the Wind Atlas for Egypt". Along-Track Scanning Radiometer (ATSR) data from the European Remote Sensing Satellite (ERS) have been used to map the sea- and land-surface temperatures and albedos.

Copies to: Information Service Department (2)